Journal of Innovations in Computer Science and Engineering
Shahid Beheshti Unversity

January 2024, Volume 1, Issue 2

Beyond Six Degrees of Separation: Exploring Milgram's Condition in Complex Networks

F. Safaei[1]✉, **ORCID:** 0000-0002-8546-3148
M. R. Sadeghi[2], **ORCID:** 0009-0000-1782-9155
M. M. Emadi Kouchak[3], **ORCID:** 0009-0009-2572-3356
[1] Faculty of Computer Science and Engineering, Shahid Beheshti University, Tehran, Iran f_safaei@sbu.ac.ir,
[2] Faculty of Information Technology and Electrical Engineering, University of Oulu, Oulu, Finland
mohammadreza.sadeghi@student.oulu.fi,
[3] Department of Computer Engineering, Science and Research Branch, Islamic Azad University, Tehran, Iran
m.m.emadi@srbiau.ac.ir

Abstract -The concept of six degrees of separation stands as a significant phenomenon, positing that any two independent entities worldwide can connect through a chain of no more than six acquaintances. This article delves into the study of this phenomenon across various network models, aiming to quantify the rates of information propagation, idea dissemination, disease transmission, and predictive trends in society and economics. We extend the examination beyond the conventional notion of "six degrees of separation" by investigating the factors impacting degrees of separation and Milgram's condition in complex networks. Our objective is to elucidate that the actual degree of separation within a network is intricately tied to its structure and various parameters. Instead of being a universal rule, this concept can be construed as a condition that networks must satisfy. We explore Milgram's condition in diverse network models, encompassing random, small-world, and scale-free networks, while scrutinizing the impact of the frequency and length of cycles on degrees of separation. Additionally, we analyze the correlation between different network parameters, including the clustering coefficient, degree distribution, heterogeneity, scaling exponent, and probability of rewiring, with Milgram's condition. We introduce a novel criterion, termed multiplicity within the network and assess its relationship with the Hamming distance. We evaluate the effectiveness of Milgram's condition and degrees of separation in the context of these two parameters. Our findings underscore the close association between Milgram's condition and degrees of separation with the specific network model and its structure. Consequently, through computational analyses and numerical simulations on diverse network models, this article aims to provide a comprehensive understanding of the underlying mechanisms governing degrees of separation and Milgram's condition in complex networks. The insights gleaned from this research are invaluable for network design and optimization, offering a deeper comprehension of complex network properties

Keywords: Milgram's Condition, Six Degrees of Separation, Small-Worldness, Hamming Distance, Network Multiplicity, Complex Networks, Graph Theory

1. Introduction

Complex networks have emerged as a fascinating and rapidly growing field of research, garnering considerable attention in recent years across various academic domains, including physics, mathematics, computer science, biology, and social science. These networks constitute an assembly of interconnected elements, such as nodes or agents, capable of representing an extensive array of real-world systems, encompassing social networks, transportation systems, biological structures, and technological infrastructures. The study of complex networks holds profound significance due to its potential to furnish a robust framework for comprehending the behavior, structure, and dynamics inherent in these multifaceted systems.

Complex networks offer a potent avenue for modeling and analyzing a diverse spectrum of phenomena, including the spread of diseases, the emergence of social communities, the intricate architecture of the Internet, the intricate workings of the human brain, and more. Additionally, delving into complex networks has yielded the development of novel mathematical and computational tools, including network analysis, graph theory, and statistical physics. These tools serve as invaluable instruments for gleaning profound insights into the structures and dynamics of intricate systems, while concurrently paving the way for innovative applications across diverse domains such as medicine, economics, and engineering.

The concept of "six degrees of separation" stands as a significant phenomenon, positing that any two independent entities worldwide can be connected through a chain of six or fewer acquaintances. This notion was first introduced by Hungarian writer

Submit Date: 2024-10-15
Revise Date: 2025-03-09
Accept Date: 2025-03-12
✉ Corresponding author

Frigyes Karinthy [1] in 1929 and gained prominence in the 1960s through the pioneering experiments conducted by Stanley Milgram [2]. Milgram's experiments involved randomly selecting individuals and tasking them with sending a letter to a target person residing in a different region of the country, solely relying on the chain of intermediate acquaintances for delivery. Although Milgram's experiments demonstrated that the average number of intermediate acquaintances is small, typically around six, the validity of the concept of six degrees of separation has faced scrutiny in subsequent years. Some rigorous critics have contended that these experiments may suffer from sampling biases, casting doubt on the generalizability of their findings to larger populations. However, the resurgence of interest in the study of complex networks has reignited the investigation into the phenomenon of six degrees of separation and Milgram's condition.

The Small-World model, introduced by Watts and Strogatz in 1998 [3], stands as another prominent example within the realm of complex networks. This model finds its foundation in the remarkable interplay of high clustering and short distances between nodes. Recent research has unveiled that the concept of six degrees of separation is not limited solely to small-world networks; it can be expansively applied to other models as well, notably scale-free networks, characterized by their power-law distribution of node degrees. Examining the problem of degrees of separation and Milgram's condition across different network models holds paramount importance on several fronts. First, it serves as a beacon, illuminating the robustness and performance dynamics of real-world communication networks. Second, it lays the groundwork for devising efficient routing strategies and optimal search algorithms, facilitating seamless information propagation within complex networks. Lastly, this multifaceted exploration augments our understanding, offering deeper insights into the fundamental principles that govern the emergence and evolution of complex networks.

Further, this investigation holds the potential to elucidate the pace at which information, ideas, and diseases spread, along with its implications for societal and economic trends. To illustrate, comprehending the degrees of separation between individuals facilitates the identification of pivotal figures or influencers within social networks. These individuals possess the capacity to rapidly disseminate ideas or products to a vast audience. Similarly, a study of degrees of separation between cities or distinct regions can unveil critical hubs and bottlenecks, offering valuable insights for optimizing transportation and resource allocation. In communication networks, a nuanced understanding of this aspect between different nodes lays the foundation for enhancing information routing algorithms and augmenting network performance.

Notably, within the realm of online social networks, this exploration has catalyzed advancements in the design and implementation of information exchange and recommendation algorithms, enhancing user experience and engagement. In summation, the investigation into degrees of separation and Milgram's condition within complex networks holds the promise of providing profound insights into network structure and performance. Its diverse and pragmatic applications span fields as varied as social networking, transportation, and communication, underscoring its significance in contemporary engineering and beyond.

Within this study, our objective is to demonstrate a significant correlation between Milgram's condition and the actual value of degrees of separation within a network, considering the network's structure and various influencing factors and parameters. We seek to emphasize that this value may not consistently align with the classical notion of six degrees of separation. Instead, it should be perceived as a conditional threshold within a network, subject to the network's unique characteristics.

In this manuscript, we delve into the exploration of Milgram's condition across diverse network models, encompassing random, small-world, and scale-free architectures. Our investigation delves into the impact of cycles with varying lengths and frequencies on degrees of separation while scrutinizing their relationships with network statistics. Further, we delve into the effect of the possibility of rewiring within the small-world network model on both Milgram's condition and degrees of separation. We also introduce a novel criterion named "frequency" and examine its relationship with this phenomenon through discussions of the Hamming distance.

The manuscript is structured into six sections to facilitate a coherent presentation of our findings. Section 2 provides a succinct overview of essential definitions and background information necessary to comprehend subsequent sections. In Section 3, we offer a brief review of related work in the field. Section 4 presents an in-depth exploration of the degrees of separation problem and Milgram's condition. In Section 5, we present numerical results stemming from simulation experiments. Finally, in Section 6, we conclude our findings and offer insights into potential future research directions.

2. Related Work

In 1967, Stanley Milgram conducted his iconic experiment to investigate the social phenomenon known as "six degrees of separation" [2]. His model posited that any two individuals worldwide could be connected through a chain of acquaintances comprising no more than six intermediate people. While the validity of the six degrees of separation hypothesis has faced significant scrutiny and criticism in recent years, the core idea remains a captivating concept that continues to inspire numerous researchers in the field of network science. For instance, in Facebook's 2016 experiment [8, 9], an approximate median value of 100 was calculated for the distribution. This implies that nearly 50% of Facebook users have approximately 100 acquaintances or friends. It is worth noting that this number may appear somewhat imprecise due to distribution skewness. In a 2011 experiment, Facebook reported this number to be approximately 190, and the average degrees of separation on Facebook were documented as 4.74 [9, 10]. Subsequently, in 2016 measurements when Facebook boasted 171 billion members [8-10], this number decreased to 3.75.

The concept of the small-world phenomenon was initially introduced by Watts and Strogatz [3], receiving considerable attention within the scientific community. They put forth a straightforward mathematical model capable of generating networks characterized by both a low average distance and high clustering coefficients. Subsequent to their pioneering work, a multitude of studies have been undertaken to explore the properties of small-world networks and their implications across various domains, encompassing social networks, communication networks, biological systems, and more.

Neumann [11] also presented a model of the small-world phenomenon, which serves as a modified rendition of the Watts-Strogatz model. In Neumann's model, edges are not rewired; instead, new edges are introduced to ensure network connectivity. In essence, pairs of nodes are randomly chosen, and shortcut edges are incorporated between them. It has demonstrated that the average distance or separation between nodes (referred to as the *q*-degree of separation) can be calculated using the following relationship [11]

$$< q >\approx \frac{2N}{< k >} F(N\alpha < K > /2) \quad (1)$$

where the function *F*, for small values of the rewiring probability α, can be expressed using the following e [11]:

$$F(x) \approx \frac{1}{2\sqrt{x^2+2x}} \text{tgh}^{-1}\sqrt{\frac{x}{x+2}} \quad \text{;for small } \alpha \quad (2)$$

Many studies have delved into the intricate interplay between Milgram's condition and various properties of network models. For instance, some investigations have scrutinized the pivotal role of weak ties and bridging nodes in facilitating communication across disparate segments of a network [3, 6, 11]. Additionally, other research endeavors have focused on unraveling the influence of clustering coefficients, scaling exponents, and rewiring probabilities on the small-world effect. However, substantial uncharted territory remains, awaiting exploration. One such unexplored realm centers on the role of cycles, their length, and frequency in shaping Milgram's condition and the degrees of separation within networks. Moreover, factors like the multiplicity criterion and the Hamming distance, which have not received thorough examination in the context of Milgram's condition and degrees of separation, will be meticulously explored. Consequently, the current study endeavors to investigate these dimensions comprehensively, aiming to yield deeper insights into the intricate relationship intertwining network statistics, Milgram's condition, and degrees of separation.

More recent studies have further refined our understanding of the small-world effect. For instance, Bringmann, Karl, et al. [12] explored decentralized greedy routing in geometric inhomogeneous random graphs (GIRGs), a model that addresses the limitations of prior models in explaining small-world dynamics. Their findings demonstrated that greedy routing in GIRGs succeeds with constant probability, achieving near-optimal path lengths of Θ(loglogn), thereby providing a theoretical underpinning for Milgram's experimental observations.

Another recent study by Famian [13] investigated the small-world phenomenon within the urban linguistic landscape of Tehran's Vanak Square. Their research analyzed multilingual signage and spatial-institutional references to demonstrate how linguistic networks contribute to and reinforce small-world effects in urban settings. This socio-semiotic perspective extends the small-world concept beyond traditional social networks and into linguistic and cultural frameworks.

Similarly, T. Goodrich et al. [14] proposed a new approach by modeling the small-world phenomenon in road networks rather than abstract social structures. Their Neighborhood Preferential Attachment (NPA) model integrates geographic proximity with preferential attachment, outperforming previous models in simulating efficient message routing and replicating Milgram's six degrees of separation under realistic dropout rates. This advancement highlights the role of geographic constraints in shaping small-world connectivity.

Furthermore, Schnettler [15] provided a historical and conceptual overview of small-world research in the Handbuch Netzwerkforschung, tracing its evolution from a sociological observation to a core topic in complex network theory. Their work highlighted both methodological successes and inherent limitations in small-world studies. Meanwhile, Jiang Wu [16] reviewed classic and extended small-world models (Watts-Strogatz, Watts-Strogatz-Kleinberg), applying them to empirical datasets such as the World Wide Web and an online medical community to analyze the impact of network structure on information dissemination.

These recent contributions illustrate the continued relevance and expanding scope of small-world research, reinforcing its applicability across diverse disciplines. By incorporating newer models and empirical analyses, these studies address previously overlooked aspects such as routing efficiency, linguistic connectivity, geographic constraints, and real-world verification of theoretical models. In light of these advancements, our study builds upon both classic and contemporary findings to further explore the mechanisms underlying small-world connectivity in complex networks.

3. Milgram's Condition and *q*-degree of Separation

We previously discussed the concept of six degrees of separation or the small-world property, which implies that regardless of a person's location in the world, they can establish a path with a maximum length of six connections to reach any of their friends. In simpler terms, even an individual with a modest number of acquaintances can establish a connection with someone on the opposite side of the globe. In the context of a random network, the average degree denoted as <*k*> signifies that a node within the network can directly reach <*k*> other nodes in one hop, <*k*>(<*k*>–1) nodes in two hops, and eventually engage in message and information exchange with $< k > (< k > -1)^{q-1}$ other nodes in *q* hops. Nevertheless, it is important to note that the number of nodes within a network at a distance of *q* hops, denoted as *N*(*q*), cannot exceed the total number of network nodes, *N*, since *N*(*q*) cannot exceed *N*. This implies that distances within the network cannot assume arbitrary values. In other words, $N \square < k > (< k > -1)^{q-1}$. Consequently, when calculating the number of nodes located at a distance of *q* hops from the origin node, based on the principles of geometric progression, we arrive at the relationship $N(q) \square (< k >^{q+1} -1)/(< k > -1)$. If we consider $q_{\max}$ as the representation of the network's diameter, then for k ? 1, $N(q_{\max}) \square < k >^{q_{\max}} \square N$; hence, the diameter of a random network approximately equates to $\ln N / \ln < k >$ [6]. This criterion can serve as a basis for comparing different network models, although more refined approximations will be introduced in Section 4.

All of this underscores the idea that the network diameter encompasses a small number of paths spanning a considerably large distance. In random networks, these distances tend to be significantly smaller than the overall network size, such that $\ln N \square N$. In the small-world phenomenon, the diameter of the network does not hinge on its size or its powers but is instead reliant on the natural logarithm of the network's size. It is evident that as a network becomes denser, the average distance within it diminishes.

Milgram's condition posits that if a person has k acquaintances, then the number of her/his friends and indirect acquaintances can be approximated as

$$N = \sum_{i=0}^{q-1} k(k-1)^i = k(k^{q-1}-1)/(k-1) \approx k^q \quad (3)$$

In this equation, the parameter q signifies the distance or separation number, denoting the number of steps one must traverse to transmit messages and information to k^q other individuals via intermediary acquaintances. It is important to note that, in Milgram's experiment, this condition necessitated that participants were solely permitted to convey messages to individuals they personally knew—be it a friend, family member, or any other close acquaintance. These were individuals deemed to have a meaningful relationship with the target person [3, 6, 11]. Participants were instructed to persist in this process of message transmission throughout their social network until the message ultimately reached the target person. Milgram's findings revealed that, on average, the number of intermediate acquaintances involved in this process was approximately 6, giving rise to the renowned concept of "six degrees of separation." Notably, Milgram's condition did not explicitly establish a direct correlation between the size of one's social network and the degree of separation between individuals. However, his small-world experiment suggested that even within a large population, there exists a relatively small number of intermediate acquaintances (degrees of separation), typically estimated to be around 6, connecting any two individuals.

It is worth noting that the network of friends and acquaintances, in practical terms, often resembles a tree structure and lacks cycles. Besides, it may not necessarily exhibit a high clustering coefficient. Additionally, it is important to recognize that acquaintance and friendship typically entail a symmetrical relationship. However, in real-world networks, we encounter structures with cycles and notably high clustering coefficients. Due to the presence of clustering and cyclic structures, particularly those with a length of three or more, the effective size of the community of individuals (denoted as N) often fails to reach an extensive value. Consequently, the degrees of separation within such networks tend to be less than 6. Hence, the primary objective of this article is to delve into the intricate relationships between degrees of separation, clustering coefficients, and various other statistical metrics and parameters of the network. Equation (3) hints at the existence of a power-law relationship between an individual's community size (N) and the degrees of separation (q). This suggests that the size of an individual's community network is proportionate to the number of acquaintances they possess raised to the power of the degree of separation.

However, it is important to acknowledge that the size of an individual's social network and the degrees of separation among individuals within a society can be intertwined in complex ways. Generalizations regarding this relationship can be challenging without considering the specific context and societal nuances under investigation. Moreover, numerous factors such as geographical, cultural, and technological considerations exert influence on the structure and integration of social networks, adding layers of complexity to this relationship.

3.1 The Impact of Various Network Statistics on Milgram's Condition and the Degrees of Separation

In this section, we embark on an in-depth exploration of the challenges posed by degrees of separation and Milgram's condition within various models of complex networks. Our investigation spans multiple dimensions and criteria to provide a comprehensive understanding. We delve into the intricate relationships between degrees of separation and several network statistics, including average clustering coefficient, generalized clustering coefficient for Cycles of varying lengths. We scrutinize the role and impact of cycles in the network, particularly those with different lengths, on the small-world property and degrees of network separation. This entails investigating whether the frequency of cycles and specific patterns, along with their respective lengths, significantly influence the small-world effect and degrees of separation. Moreover, we assess the issue of information propagation rate and its correlation with degrees of separation, taking into account the impact of different network topologies on this phenomenon.

At the outset of this section, we address a fundamental question; what is the impact of cycles and motifs of varying lengths on the small-world phenomenon and the degrees of network separation. This inquiry probes whether the frequency of cycles and specific patterns, along with their lengths, substantially affect the small-world effect and degrees of separation within the network. Notably, the relationship between degrees of separation and the clustering coefficient in a complex network is not static but varies based on network characteristics. Networks characterized by high clustering coefficients tend to exhibit shorter paths and, consequently, lower degrees of separation. Conversely, networks with lower clustering coefficients may experience a higher degree of separation. The clustering coefficient measures the tendency of nodes in the network to form clusters and groups. A higher clustering coefficient signifies that nodes are more likely to share mutual neighbors, facilitating efficient information transfer through local connections and clusters. This, in turn, leads to shorter path lengths and a reduction in degrees of separation.

The speed of information propagation within a network is influenced by a multitude of factors, including degrees of separation, network size, average degree, clustering coefficient, network heterogeneity, and more. The rate of information propagation within a network can be roughly approximated by the equation $R = N / T$, where N represents the network size, and T stands for the average time required for information to traverse between two nodes. The time needed for a message to reach another node is contingent on the number of links it traverses. If a node maintains an average of $<k>$ links, it can simultaneously transmit messages to $<k>$ other nodes. Consequently, the time taken for a message to reach neighboring nodes is inversely proportional to $1/<k>$. Thus, the parameter T is proportionate to $1 / \lambda$, where λ represents the rate at which a node can establish contacts per unit of time. In the context of q-degree of separation, this rate can be expressed as $\lambda = 1/(\tau < k >^q)$, where τ denotes the average time needed

to establish a contact. Typically, τ is assumed to be equal to unity for a unit-length walk. Therefore, the speed (rate) of information propagation, *R*, can be expressed in terms of the *q*-degree of separation within a network of size *N*, with an approximate formula $R = N/ < k >^q$.

It is important to note that network performance evaluation encompasses three primary categories of criteria. (1) Local structure criteria: This category includes criteria related to the local structures around nodes. Examples of such criteria comprise average degree, edge density, degree heterogeneity, clustering coefficients, modularity index, average geodesic distance, and average node betweenness. (2) Walk-based criteria: In contrast to the first category, these criteria consider information transmission not only through short paths but also through any accessible path connecting corresponding pairs of nodes. These criteria rely on the concept of walks rather than paths. Examples within this category encompass eigenvector centrality, subgraph centrality, and average communicability. (3) All-walks index criteria: This third group of criteria is founded on the all-walks index, which assigns less weight to longer walks between node pairs. Typically, criteria in the second category account for all routes connecting nodes but penalize relatively lengthy routes. To incorporate longer walks into the analysis, Estrada [17, 13] proposed a measure $Z = \sum_{q=0}^{\infty} A^q / q!!$ for the adjacency matrix *A*. In this measure, walks of length *q* are penalized by q!! (double factorial). The *Z* matrix, derived from the underlying graph, computes the average of elements situated on the main diameter (i.e., $< Z_{ii} >= (\sum_{i=1}^{n} Z_{ii}) / n$). This contribution of a node like *i* to all subgraphs of the graph includes larger subgraphs compared to the subgraph centrality criterion. Moreover, one can average all elements of the *Z* matrix, considering $< Z_{ij} >= \frac{2}{n(n-1)} \sum_{i,j} Z_{ij}$ as a measure of the network's global capacity to transmit information between pairs of nodes. Consequently, this enables information transmission over longer distances.

In our experimental outcomes (detailed in Section 4), our observations indicate that the *Z*-Estrada index [17], compared to the *R*-index (representing information propagation rate), more effectively quantifies the level of communicability and the network's aptitude for information propagation—a pivotal characteristic of the small-world phenomenon.

Several network characteristics play a pivotal role in influencing both Milgram's condition and the degrees of separation within the network. For instance, denser networks characterized by a multitude of connections between nodes tend to exhibit shorter paths and reduced degrees of separation. Conversely, networks with skewed and heterogeneous degree distributions may result in longer paths and higher degrees of separation. These scenarios will undergo thorough investigation and analysis in our simulation experiments.

In the remainder of the article, in our quest to provide a quantitative assessment of the small-world property and Milgram's experiment, it becomes essential to precisely define Milgram's condition and the degrees of separation within the network. To achieve this, we must engage in manipulation of the adjacency matrix of the graph, which contains crucial information pertaining to its structural makeup. In pursuit of this objective, we introduce the R^p matrix, derived from the adjacency matrix of the graph, denoted as *A*. This matrix is defined as [19]

$$[R^p]_{i_0,i_p} = \sum_{i_1 \sim i_{p-1}} \prod_{\substack{0\le k\le p-1, 1\le l\le p \\ k\neq l}} a_{i_k,i_l} \prod_{\substack{i_k,i_j \\ i_k - i_j > 1}}^{p} (1-\delta_{i_k,i_j}) \qquad (4)$$

In the equation above, R^p is a matrix where element *(i, j)* represents the number of non-repeating paths of length *p* between nodes *i* and *j*. The term within the sigma summation operator calculates the number of such paths. To form a path of length *p*, it is necessary to have (*p*–1) nodes located between the source and destination. Consequently, the sigma summation traverses all possible combinations of nodes, considering (*p*–1) nodes.

Within the sigma expression, there is expression $\prod_{\substack{0\le k\le p-1, 1\le l\le p \\ k\neq l}} a_{i_k,i_l} = a_{i_0,i_1} a_{i_1,i_2} \ldots a_{i_{p-1},i_p}$ so that a_{i_i,i_j} signifies the entry located at index (*i*, *j*) in the adjacency matrix, *A*, of the graph. If its value equals one, it indicates the presence of an edge between node *i* and *j*. In this context, if all $a_{i_0,i_1} a_{i_1,i_2} \ldots a_{i_{p-1},i_p}$ values equal one, it implies the existence of a path from the starting node i_0 to the end node i_p, traversing nodes i_0, i_2,…, i_p, respectively.

Now, to ensure the absence of cycles in a path of length *p*, it is essential to verify that none of the edges along i_0, i_2,…, i_p are repeated. For this purpose, the condition $\prod_{\substack{i_k,i_j \\ i_k - i_j > 1}}^{p} (1-\delta_{i_k,i_j})$ is employed, wherein the δ_{i_k,i_j} expression implies Kronecker's delta. Kronecker's delta assigns a value of 1 when i_k equals i_j, and it equals 0 in all other cases. Consequently, the $\prod_{\substack{i_k,i_j \\ i_k - i_j > 1}}^{p} (1-\delta_{i_k,i_j})$ condition checks that each *k* and *j* index in i_0, i_2,…, i_p is unique, ensuring that no nodes are repeated. Additionally, the condition $i_k - i_j > 1$ stipulates that *k* and *j* must be distinct from each other; as $\exists\, i_i = i_k$, would signify the repetition of a node in traversing a path of length *p*. In such cases, $1-\delta_{i_k,i_j} = 0$, and when multiplied by the remaining expression, the total value within the sigma summation becomes zero. In essence, this means that the desired path is excluded from the calculation of R^p.

Safaei and his coauthors [20] have presented a relationship that expresses graph energy [21] based on the largest eigenvalue of its adjacency matrix, often referred to as the spectral radius. Their proposed expansion relies on the even powers of the adjacency matrix. They have demonstrated that the powers p of the trace of the adjacency matrix, denoted as $\mathrm{tr}A^p$, can be employed to compute the number of closed walks of length p—where p can be either even or odd. These closed walks correspond to specific subgraphs within the graph structure. To illustrate, $\mathrm{tr}A^2$ calculates the number of closed walks of length 2, which corresponds to graph edges, while $\mathrm{tr}A^4$ yields closed walks of length 4, encompassing cycles of length 4. As the powers increase, additional subgraphs emerge. For instance, the cycle C_8 first appears in $\mathrm{tr}A^8$. Consequently, a key aspect we will delve into further is the influence of the quantity and frequency of subgraphs and cycles in various network models on Milgram's condition and the degrees of separation. This is crucial due to the substantial impact of cycles, graphlets, motifs, and closed walks on network properties such as average distance, spectral values, heterogeneity, information propagation rate, and, in essence, any factor linked to network degrees of separation.

By calculating the matrix R^p using Equation (4), and aligning with the concept of powers p from the trace of the adjacency matrix, as previously discussed, we can define the p^{th} clustering coefficient within the network as [19]

$$C_p = \frac{\mathrm{tr}\, R^p}{\sum_{i,j} R^{p-1}} \tag{5}$$

In the equation above, the numerator of the fraction signifies the number of cycles of length p—starting from the initial node and returning to itself after traversing p hops (edges). However, in the denominator of the fraction, we calculate the number of connected p-plets within the entire graph. In cases where these p-plets are not interconnected, only $(p-1)$ hops (edges) are taken into account. The inclusion of the sigma summation in the denominator of the fraction entails a summation over all elements of the R^{p-1} matrix or the total number of $(p-1)$ nodes connected to each other. It is worth noting that this division normalizes the generalized clustering coefficient parameter in the graph to fall within the interval [0,1].

Consequently, the p^{th} generalized average clustering coefficient within a network can be expressed as

$$\bar{C}_p = \frac{p \cdot C_p}{S_p} \tag{6}$$

Where p represents the length of the cycle, C_p denotes the number of cycles comprising p edges, and S_p indicates the quantity of connected p-plets in the underlying network. This parameter is defined for the square adjacency matrix, A, with N^2 elements, derived from the summation over all elements of the matrix R matrix raised to the power of $(p-1)$, given by

$$S_p = \frac{1}{2}\sum_{i,j} R^{p-1} \tag{7}$$

As previously mentioned, S_p in Equation (6) represents the number of walks of length p (comprising $(p-1)$ nodes). These walks encompass connected p-plets, which may either be closed (forming a cycle) or open (constituting a path graph). Importantly, these walks are non-repetitive, meaning they lack cycles and multiple links. Additionally, there are no closed walks within them. In other words, they may be closed, signifying that the starting and ending nodes are connected, but they do not contain any closed circuits or loops.

It is worth noting that the coefficient "1/2" in Equation (7) is employed to avoid double counting since walks of length p can be calculated from both directions, both of which are essentially the same, representing a single unique walk.

The clustering coefficient parameter $\bar{C}_p$ in Equation (6) serves as a metric for assessing the tendency of network nodes to form p-cliques or cycles of length p. The relationship between $\bar{C}_p$ and the degrees of separation is the focal point of our investigation. However, it is essential to acknowledge that this relationship depends on a multitude of factors, including network size, structure, node degree distribution, the value of p, and more. Generally, higher values of $\bar{C}_p$ indicate a greater tendency for the network to possess shorter paths and lower degrees of separation. Consequently, the flow of information traversing the network can move through local clusters and cycles more swiftly and efficiently.

To enumerate the number of connected p-plets (the sets comprising p connected nodes), we must tally such sets within the network. It is important to note that this calculation exhibits high computational complexity, particularly for larger network sizes. Hence, techniques like Monte-Carlo simulations or sampling can be employed to estimate the quantity of such connected p-plets [21].

Clearly, when p is set to 3 in Equation (6), we arrive at the well-known Watts-Strogatz clustering coefficient [3]. In essence, Equation (6) represents a further development and generalization of this coefficient. Therefore, in this article, it is referred to as the *generalized clustering coefficient*. It is worth mentioning that the Watts-Strogatz clustering coefficient, expressed in terms of the trace of the power of 3 of the network adjacency matrix (signifying the number of triangles), can be articulated as

$$\bar{C}_3 = \frac{\mathrm{tr}A^3}{\sqrt{\sum_{i,j} a_{i,j}^2} - \mathrm{tr}A^2} \tag{8}$$

where a_{ij} corresponds to the entry in the i^{th} row and j^{th} column of the adjacency matrix A. Additionally, the Watts-Strogatz clustering coefficient can be expressed as follows, incorporating the rewiring probability α (which involves swapping edges in the network) and the network's average degree

$$\bar{C}_3(\alpha) = \frac{3}{4} \cdot \frac{< k > -2}{< k > -1} \cdot (1-\alpha)^3 \tag{9}$$

The above equation can be interpreted as follows. The first part implies the clustering coefficient in a regular lattice, which is approximately 75% for high degrees. To interpret the second part of this equation, it should be noted that the probability that a connected triple will remain connected after rewiring is equal to the probability that none of these three edges will be rewired. This probability is equal to $(1-\alpha)^3$. Consequently, it is multiplied by the clustering coefficient of the regular lattice. It is worth mentioning that the probability of rewiring the edges to form a connected triplet is very small and can therefore be neglected.

The frequency of cycles and their occurrence in small-world networks can also be related to the concept of degrees of separation. Cycles have varying lengths and can emerge due to high clustering in small-world networks, thus facilitating the propagation of information and enhancing communication efficiency between nodes. Cycles can give rise to motifs and graphlets, which recur in different parts of the network. When nodes are connected through short cycles, information exchange becomes swift and efficient. This reduces the number of steps required to exchange messages between nodes and consequently diminishes the degree of network separation. Therefore, the investigation of cycles, motifs, and graphlets in various small-world network models can yield valuable insights into information dissemination and the factors influencing degrees of separation.

It is also important to note that the length of cycles or closed walks in networks plays a significant role in Milgram's condition and network degrees of separation. As the length of cycles increases, the likelihood of encountering longer and more convoluted paths also increases, resulting in reduced efficiency of information propagation and a weakening of the network separation effect. Consequently, it appears that the small-world effect and the issue of network degrees of separation primarily apply to cycles or closed walks with relatively short lengths (e.g., 6 or 7), with this effect diminishing for longer cycles.

Now, in a network of size N, Milgram's condition with q-degree of separation, denoted by the symbol M_q throughout this article, can be defined as [22]

$$M_q \triangleq \frac{1}{N} S_q \tag{10}$$

In the above relationship, S_q is the parameter calculated in Equation (7). Dividing by N signifies averaging over it, which is employed as Milgram's condition in this article. Essentially, it corresponds to the average number of walks of length q, interpreted as the q-degree of separation within the underlying network. Another interpretation can be framed as how probable it is for two randomly chosen nodes in the network to reach each other in at least q steps, or the minimum distance between them is q. It is essential to emphasize that the q-degree of separation criterion encompasses more than just the average number of q-plets in the network; it fundamentally signifies the likelihood of finding a path of length q between any two arbitrarily selected nodes within the network. The higher the numerical value of Milgram's condition, the greater the likelihood that two selected nodes can be connected via a path of length q, consequently reducing the degree of network separation.

An alternative interpretation of Milgram's condition pertains to the concept of network efficiency, specifically the extent and effectiveness of information transfer within the network. Remarkably, even when nodes appear to be distant from each other, the presence of walks, cycles, and their frequency enhances this possibility and the overall efficiency of the network. This, in turn, leads to rapid information transmission between nodes, a crucial and vital feature observed in numerous real-world networks such as viral transmission, biological networks, transportation, and communication.

Another intriguing observation to highlight is that by taking the logarithm of Milgram's condition in Equation (10), we can define a figure of merit (FoM) that quantifies the quality of communication within a network based on Milgram's condition. The use of $\log(M_q / N)$ form provides us with deeper insights into the characteristics of the underlying network. If this value equals 1, it signifies a critical situation for Milgram's condition. In other words, the number of nodes meeting at a q-degree of separation is several times greater than the network total size, N. This is a significant point, indicating that the number of nodes converging at q-degree of separation is of the same order of magnitude as the total network nodes (N), illustrating that a highly interconnected network facilitates efficient information transmission. Another interpretation suggests that this point marks the juncture where the search process in Milgram's experiment extends across the entire network, effectively scanning the network and increasing the likelihood of locating a target node. Therefore, this point can be viewed as a saturation threshold within the network, beyond which further exploration beyond q degrees of separation yields diminishing returns in terms of discovering new nodes in the network. In simpler terms, beyond the saturation point, the probability of locating the target node through random searches significantly decreases. This boundary condition serves as a crucial threshold in Milgram's condition, providing a basis for assessing the effectiveness of algorithms and search strategies. This aspect will be thoroughly examined in the numerical results obtained from simulation experiments (see Section 4).

In this context, taking the logarithm of Milgram's condition, denoted as $\log(M_q / N) = 1$, offers us a network merit criterion, shedding light on how information can propagate within q steps (degrees of separation) relative to the network size. Additionally, the median of the CDF signifies the average degree at which 50% of nodes (individuals) possess, on average, q acquaintances. When $\log(M_q / N)$ equals 0.5, it indicates that the probability of two nodes connecting to each other and exchanging information and

messages through the intermediary q acquaintances (degree of separation) is higher than 50%, almost approaching half the value of the boundary condition (saturation point) observed in the Milgram experiment.

In this article, we introduce a stochastic variable known as X_q, which corresponds to the q-degree of network separation. The definition of this random variable is expressed as a summation of the p^{th} generalized clustering coefficients, as follows

$$X_q \equiv \sum_{p\geq 3}^{q} \bar{C}_p \tag{11}$$

The interpretation of the stochastic variable X_q may signify the impact of cyclic structures with length p and ($3\leq p\leq q$) within the underlying network. It is evident that cycles with lengths of 1 and 2 ($p\geq 3$) are absent. Hence, Equation (10) provides valuable insights into the structures formed by p edges in the network. By analyzing the random variable X_q for various q values, we can collect information about the frequency distribution of cycles with diverse lengths in the network and understand how these cycles contribute to its connectivity and communication. This matter, among others, will be extensively discussed in the simulation section.

4. Numerical Results

In this section, our objective is to leverage numerical results obtained from simulations to explore the phenomenon of degrees of separation and Milgram's condition across various complex network models, encompassing random, small-world, and scale-free networks. Our goal is to evaluate network performance and conduct an in-depth analysis of these aspects.

Figure 1 presents probability density function (PDF) and cumulative distribution function (CDF) depicting network distance distributions across different network models including random, small-world, and scale-free networks. These models are defined by specific parameters; the connection probability of 0.4 for the random model, a scaling exponent, γ=2.5 for the scale-free model, and the rewiring probability, α=0.3 for the small-world model. The network size remains constant at 100 nodes.

In the random network (Erdős–Rényi model [7]), the PDF exhibits a prominent peak at the average distance and subsequently experiences an exponential decline as distances diverge from the mean. Analysis of the CDF reveals that roughly 50% of network nodes maintain connections at this average distance. For the Small-world network, characterized by a rewiring probability of 0.3, the PDF showcases a pronounced peak at the minimum distance, followed by a rapid decrease with increasing distance. The thinner tail of the distribution signifies the presence of long-range connections, conforming to a power-law pattern.

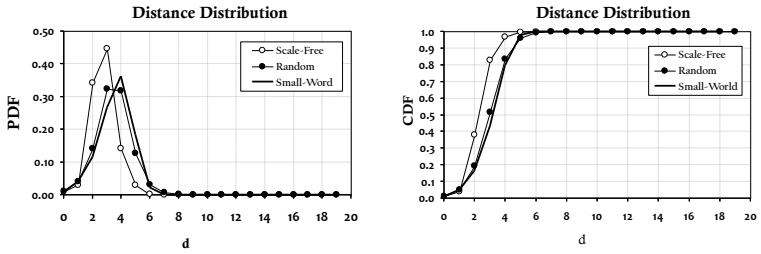

Figure 1: The Probability Density Function (PDF) and Cumulative Distribution Function (CDF) of distances in different network models including a random model network with a probability of connection set to 0.4, a scale-free model with a scaling index, γ, of 2.5, and a small-world model with a rewiring probability, α, of 0.3. The network size in this simulation is fixed at 100 nodes.

In the scale-free network, featuring a scaling exponent of 2.5, the PDF follows a power-law distribution. The lower rate of decay compared to the small-world model results from the presence of sizable hubs and clusters containing highly connected nodes, thereby facilitating efficient communication throughout the network. It is noteworthy that the Barabási-Albert model [3-6], a specific scale-free variant, exhibits a distance distribution with its peak at the maximum distance ($d_{\max}$), and a heavy tail indicating the prevalence of hubs and long-range connections.

These observations underscore the critical role of diverse network statistics, including average degree, rewiring probability, growth rules, preferential attachment [6], and scaling exponents. Such analyses emphasize the need to consider multiple criteria to gain a comprehensive understanding of network degrees of separation and Milgram's condition. Additionally, these insights extend beyond the specific parameter values discussed here, offering generalizable findings applicable to various scenarios.

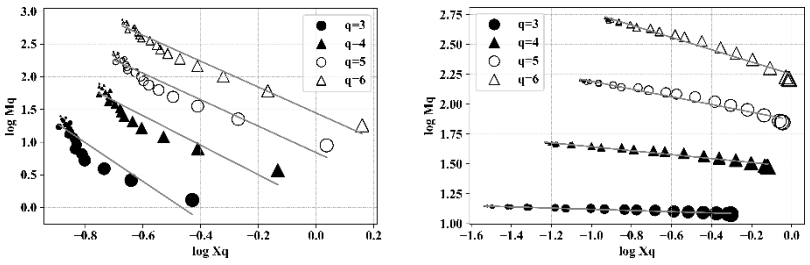

Figure 2: The linear relationship between Milgram's condition and the stochastic variable *Xq* (the sum of generalized clustering coefficient values) within the small-world network model. Both the horizontal and vertical axes are plotted logarithmically; (a) Milgram's condition is analyzed concerning network size, ranging from 10 to 200 nodes, with a fixed rewiring probability α=0.3. The data points are derived from 30 networks; (b) Milgram's condition is evaluated while keeping the network size fixed at 100 nodes, and the rewiring probability α is varied within the range [0.001, 0.5]. Thirty networks are considered for this analysis.

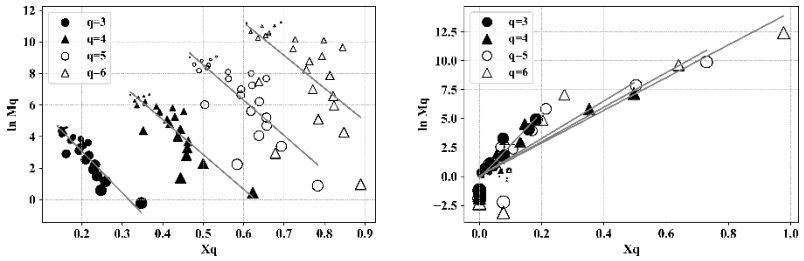

Figure 3: The exponential relationship between Milgram's condition and the random variable X_q (the sum of generalized clustering coefficient values) within the scale-free network model. The vertical axis is in natural logarithm. Two scenarios are presented; (a) Milgram's condition is examined concerning changes in network size, ranging from 10 to 130 nodes, with a fixed scaling exponent γ= 2.5. Data points are generated from 30 networks; (b) Milgram's condition is assessed while maintaining a fixed network size of 100 nodes and varying the scaling exponent, $\gamma \in$ [0.1, 10]. Again, 30 networks are considered for this analysis.

In Figure 2, Milgram's condition is presented in relation to the X_p random variable within the Watts-Strogatz small-world model [3]. The details of the model's specifications are provided in the article. Both axes in the figure are displayed on a logarithmic scale, and the data is based on 30 networks. Two specific scenarios are considered. The first subplot, 2(a), showcases Milgram's condition as a function of network size, varying from 10 to 200 nodes, while keeping the rewiring probability α constant at 0.3. In the second subplot, 2(b), Milgram's condition is depicted concerning changes in rewiring probability α, ranging from 0.001 to 0.5, with the network size fixed at 100 nodes.

In this network model, an interesting observation emerges. As the length of cycles (i.e., degrees of separation) increases from 3 to 6, there is a noticeable rise, indicating a linear relationship akin to a power-law phenomenon. This suggests that an increase in the contribution of generalized clustering coefficients within the networks corresponds to an increase in the degrees of separation, which in turn weakens Milgram's condition.

As previously mentioned in Section 3, the line represented by $y = \log(M_q / N) = 1$ corresponds to the boundary condition or saturation point of Milgram's condition. This boundary condition is met for degrees of separation $q \geq 4$. In essence, in the small-world network model, Milgram's condition is satisfied within networks characterized by cycles of length 4 to 6. The fulfillment of Milgram's condition in small-world network models conforms to a power-law relationship can be described by

$$M_q \approx B(X_q)^{-\zeta} \quad B, \zeta > 0 \tag{12}$$

where B and ζ are positive constants.

Indeed, as demonstrated by the plots in Figure 2, this relationship is grounded in a power-law framework. When expressed in logarithmic form, it exhibits linearity characterized by a positive intercept coefficient and a negative slope. As the length of cycles (i.e., degrees of separation) increases, a linear relationship emerges, reflecting the heightened contribution of generalized clustering coefficients within the network. Consequently, we can model the topological relationship of the Milgram's condition parameter, M_q, in terms of X_q in the small-world model using Equation (12).

In contrast, in scale-free networks, the presence of longer cycles and their relative frequency exhibits an exponential relationship with Milgram's condition, as articulated by the following equation

$$M_q \approx e^{bX_q} \quad b > 0 \tag{13}$$

where b is a positive constant. This observation was further validated through simulations conducted on scale-free networks, as illustrated in Figure 2.

Figure 3(a) displays the variation of Milgram's condition concerning network size, ranging from 10 to 130 nodes, while assuming a scaling exponent γ of 2.5. In Figure 3(b), Milgram's condition is plotted against changes in the γ within the interval [0.1, 10], while maintaining a fixed network size of 100 nodes. Each subplots 3(a) and 3(b) is based on thirty networks generated for analysis.

The findings presented in Equations (12) and (13) demonstrate the logical connection between Milgram's condition and the topological characteristics of the network. It is important to note that the precise mathematical form of this relationship may vary depending on the specific network type and model. Determining the exact form of this relationship necessitates in-depth mathematical analysis and empirical evidence. Additionally, the association between M_q and X_q is influenced by the distribution of X_q values across the network, which, in turn, is linked to the network's topological attributes.

In the case of small-world networks characterized by high clustering and short paths, we anticipate that X_q values will exhibit a significant skew, meaning that only a few nodes will possess high values. Consequently, in such networks, Milgram's condition is expected to exhibit a power-law relationship with X_q. In contrast, in scale-free network models with highly heterogeneous degree distributions, an exponential relationship emerges between M_q and X_q, as depicted in Figure 2. This phenomenon arises due to the presence of a limited number of highly connected nodes (hubs) which exert a substantial influence on X_q. Consequently, this leads to an exponential distribution of values for the random variable X_q, as formulated in Equation (13).

The relationship between M_q and X_q can be considered as an outcome of Milgram's original experiment, which assesses the likelihood of two randomly selected nodes in the network connecting with each other through a path of q hops or fewer. As described

in Equation (11), X_q represents a stochastic variable that involves a summation of generalized clustering coefficients, reflecting the contribution of cycles ranging from length 3 to q.

Equation (12) illustrates that this summation of cycles, ranging from length 3 to q, between two randomly chosen nodes in a small-world network model exhibits a power-law behavior. The probability of encountering such cycles is directly proportional to $C_p(p+1)^{-\zeta}$, where C_p denotes the generalized clustering coefficient associated with a specific node. This coefficient signifies the proportion of closed cycles with a length of p, centered around that particular node. The parameter ζ plays a crucial role as a scaling factor governing the decay of C_p concerning p. A smaller ζ implies that longer cycles hold more significance in influencing the clustering coefficients. It is important to note that parameter q represents the maximum observable cycle length within the network.

In this context, the average (expected value) of cycles with a length of q or less between two randomly chosen nodes can be computed as

$$X_q = N\sum_{p=3}^{q}\frac{C_p}{(p+1)^{\zeta}} \tag{14}$$

Hence, the relationship outlined above defines the expected number of nodes attainable through q-degree of separation in small-world networks. The choice of the ζ parameter can be tailored to the specific characteristics of the network model, with considerations including the degree distribution and clustering level. For instance, in the case of random network models, setting ζ to zero is appropriate, as these models typically lack inherent clustering structures. In summary, Equation (14) offers a methodology to estimate the degrees of separation within a network based on its topological and clustering attributes. This approach proves valuable for comparing various network models and conducting analyses on real-world networks.

Equation (13) and the corresponding plots in Figure 3 illustrate that the relationship observed in scale-free networks differs significantly from that in small-world networks. Instead, it exhibits an exponential connection. This discrepancy primarily stems from the presence of hubs in scale-free models. In scale-free networks, there tend to be a small number of nodes with exceptionally high degrees of connectivity, and these hubs introduce distinct topological characteristics compared to random network models. Consequently, the relationship between Milgram's condition and generalized clustering coefficients in the network diverges.

Hubs, owing to their numerous connections, serve as efficient intermediaries for short paths between network nodes. This characteristic reduces the effective diameter of scale-free networks, satisfying Milgram's condition for smaller values of q. However, the prevalence of hubs also contributes to larger-than-expected generalized clustering coefficients in these networks. Hubs often serve as focal points for the formation of triangles and other cyclic network structures. These elevated clustering coefficients in scale-free networks give rise to the observed exponential relationship between Milgram's condition and X_q, which is distinct from the pattern observed in small-world network models.

Empirical observations and numerical results within scale-free networks, as depicted in Figure 2, support the conclusion that Milgram's condition exhibits an exponential decline as the parameter q increases, and this behavior is accurately captured by Equation (13). Notably, the constant coefficient b within this equation signifies the rate of decay and is contingent on the specific properties of scale-free networks.

Another plausible explanation for this observation is the heightened degree distribution heterogeneity commonly found in scale-free networks. As the degrees of separation, q, increase, this skewness in degree distribution rapidly results in a greater number of connected q-plets within the network. In essence, larger values of C_p and longer cycles become more prevalent in such networks. This phenomenon can pose challenges for information transmission over extended distances.

The exponential form presented in Equation (13) can be rationalized by considering that in scale-free networks, the number of nodes with high degrees diminishes exponentially with increasing degree values. Consequently, the number of q-plets interlinked through nodes with elevated degrees dwindles exponentially with the parameter q. This reduction in interconnected q-plets subsequently leads to an exponential decay in Milgram's condition. Mathematically, this exponential relationship between Milgram's condition and q-plets (X_q) can be effectively expressed through Equation (13).

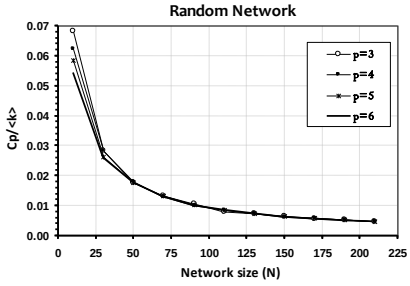

(a) Random network, Erdös–Rényi (ER) model

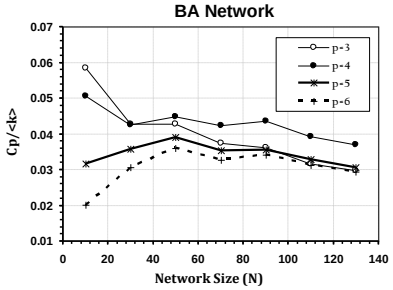

(b) Barabási-Albertt (BA) model network with a scaling exponent, γ set to 3

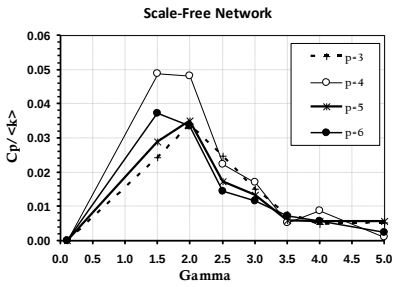

(c) Scale-free network with a scaling parameter γ typically refers to a network that follows a power-law degree distribution with a size of 100 nodes.

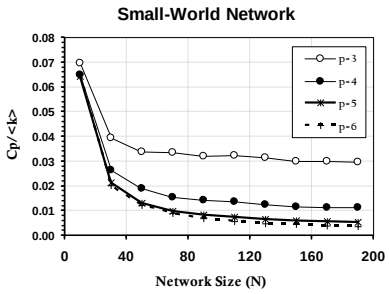

(d) Watts-Strogats small world network with rewiring probability α=0.3

Figure 4: The ratio of generalized clustering coefficients to the average network degree as a function of network size in various network models, including random networks (ER), Barabási-Albertt networks, Watts-Strogatz small-world networks, and scale-free networks. Additionally, this ratio is depicted concerning the scaling exponent, γ, in the scale-free network model. The average network degree, denoted as <*k*>, is assumed to be constant and set to a specific value.

In a random network, the clustering coefficient is related to the ratio of the average degree to the network size. As the network size increases while keeping the average degree constant, the local clustering coefficient of nodes decreases. Consequently, the average clustering coefficient of the network decreases proportionally to the inverse of the network size. To explore this phenomenon, we have created plots depicting the ratio of the average clustering coefficient to the average degree concerning network size across various network models, including random network, Erdös–Rényi (ER) model [7], Barabási-Albert model [4-6], Watts-Strogatz small-world network [3], and scale-free network [6] with different scaling exponents. When viewed from a logarithmic perspective, these plots reveal that the slope of the curves decreases as N^{-1}. In other words, the average generalized clustering coefficient also exhibits a diminishing trend with increasing network size.

In small-world networks, the influence of triangles is notably greater than that of other cycles, even as the network size increases. Among the cycles, Cycle C_6 has the least impact and contribution. In random networks, cycles generally do not exhibit significant differences in their impact or contribution, and their influence is relatively equal. However, in the Barabási-Albert (BA) model, the situation is distinct. For small network sizes, the 3-cycle structure (triangles) has a more pronounced effect. Still, as the network size surpasses a certain threshold, cycles with a length of 4 (squares) rapidly become more influential. For larger network sizes, the contribution of cycles with lengths 3, 5, and 6 becomes more comparable.

The scaling exponent parameter, γ, in the BA model is approximately 3, which aligns with the numerical results. This is a critical point in the network, as it has been observed that the average distance is proportional to $\ln(N)/\ln(\ln(N))$. However, when it comes to scale-free networks, except for the Barabási-Albert model, the role of γ in the degrees of separation phenomenon requires further examination. This will be explored in the subsequent experiments.

4.1 The Milgram's Condition and Degrees of Separation in Scale-Free Networks

In the dominion of scale-free networks, many network characteristics are contingent upon the value of the scaling exponent, γ. This parameter exhibits variability across different networks, allowing us to examine how network properties change in response to variations in γ. In most real-world networks, γ tends to be greater than 2, making values of γ less than 2 unusual. When it is less than 2, it implies that the number of links connected to the largest hub grows at a faster rate than the network size itself. For larger network sizes, this would entail that the size of the hub exceeds the total number of network nodes, which is not meaningful.

Another noteworthy observation occurs when γ is less than or equal to 2, indicating that the average degree of the network diverges as the network size increases. Consequently, the ratio of C_p (clustering coefficient) to the average degree, $C_p/\langle k\rangle$, is exceedingly small and approaches zero initially. Interestingly, under this unusual regime, the contribution of cycles with a length of 4 exceeds that of other cycles, while the contribution of triangles is less than all of them.

For values of γ between 2 and 3, we find the realm of scale-free networks. In this sort, the average distance is proportional to $\ln\ln(N)$. However, it is important to note that networks within this range are exceptionally small. Consequently, we observe a logical reduction in $C_p/\langle k\rangle$ because the network behaves similarly to small-world models, where the impact and contribution of cycles with a length of 3 (triangles) are more pronounced.

Moving beyond a γ value of 3, the effect of triangles diminishes once more, and the contribution of cycles becomes more closely tied to squares. At γ values greater than 3, the network transitions into a random regime. In this scenario, the average distance is proportional to $\ln(N)$, indicating that the degree distribution diminishes rapidly, and smaller hubs begin to dominate the network. In this context, the degree variance in the network is limited, and the average distance aligns with the characteristics of the small-world model. Although hubs still play a role in constraining distances, they are no longer of sufficient magnitude to significantly impact the distance between nodes.

From the aforementioned statements, it becomes evident that the network's topology exerts a specific influence on Milgram's condition and the phenomenon of degrees of separation. Different network models exhibit varying levels of clustering, path length,

degree distribution, eigenvalue spectra, degree heterogeneity distribution, and other factors, all of which impact the efficiency of the degrees of separation phenomenon.

This is why the investigation of degrees of separation often centers on small-world networks characterized by high clustering and an abundance of short paths. However, it is important to note that Milgram's condition can manifest in any complex network model. Nevertheless, its precise location and behavior vary from one model to another. In the case of scale-free networks featuring hubs, the phenomenon of degrees of separation necessitates a different approach. Hubs may function as bottlenecks, impeding the smooth flow of information. In situations involving hub failures or overloads, information may become trapped and fail to disseminate to other parts of the network, consequently increasing the degrees of separation between nodes. However, when compared to random networks and regular lattices, scale-free networks generally exhibit fewer degrees of separation. Conversely, networks with random and homogeneous topologies, which typically possess low clustering, may not facilitate highly efficient degrees of separation. The absence of analogous structures and local clustering can impede the efficient propagation of information throughout the network.

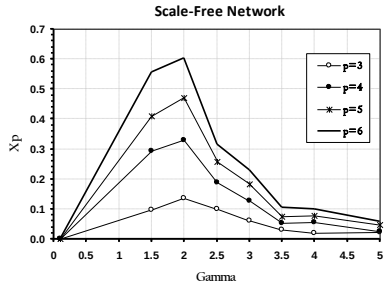

Figure 5: The contribution of cycles with lengths ranging from 3 to 6 (X_p) in scale-free network models under various values of the γ parameter. The network size is held constant at 100 nodes.

In the plots presented in Figure 5, we examine the contribution of cycles with various lengths, ranging from 3 to 6, represented as the average generalized clustering, within scale-free network models under different values of the γ parameter. As previously discussed in the explanations related to Figure 3 for scale-free networks, the characteristics of these networks are highly reliant on the scaling exponent parameter γ. When $\gamma \leq 2$, the network enters an anomalous state, where the number of links connected to the largest hub grows faster than the network size. In this scenario, it becomes evident that for γ less than or equal to 2, cycles with a length of 6 exhibit a significantly higher contribution, surpassing 80%. Conversely, triangles have the lowest contribution, amounting to roughly 20%.

Within the $2<\gamma<3$ regime, the network follows a scale-free model, and the average distance is proportional to $\ln\ln N$. In this setting, the network's behavior resembles that of the small-world model, with cycles of length 3 (triangles) exerting a greater influence and contribution. Consequently, within the $2<\gamma<3$ regime, which corresponds to the scale-free model, the contribution of cycles experiences a rapid decline and falls below 40%.

At the critical point where γ equals 3 (Barabási-Albert model), the contribution of cycles with a length of 6 reaches approximately 20%. Nevertheless, as γ surpasses 3, this contribution decreases once more. Nevertheless, larger cycles still maintain a significant contribution, with triangles contributing the least. This occurs because, under this regime, the influence of triangles diminishes. Ultimately, within the $\gamma>3$ regime, the network resides in a random model, and the average distance is proportional to $\ln N$. Hubs become smaller, and the variance in network degree is limited. While hubs are no longer sufficiently large to affect the degrees of separation, they still manage to reduce network distances.

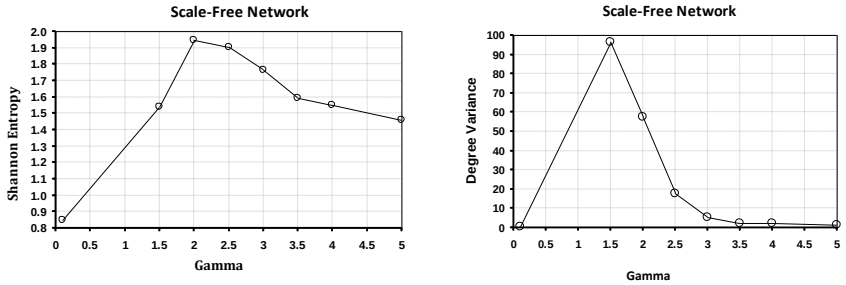

Figure 6: The network degree variance and Shannon's degree entropy in scale-free networks across different values of the scaling exponent γ. The network size is fixed at 100 nodes.

In Figure 6, we observe the variations in entropy and network degree as they relate to the scaling exponent, γ, within the scale-free network model. Entropy is a concept frequently employed in network science to quantify the level of disorder or uncertainty present in a network. Shannon's entropy, a widely recognized measure of network entropy, characterizes the randomness in the distribution of node degrees within the network. While a comprehensive examination of the relationships between various network entropies,

degrees of separation, and Milgram's condition warrants dedicated research, it is worth noting in brief that networks exhibiting greater homogeneity tend to yield higher entropy values and lower Milgram's condition values for larger q values. In such networks, an increase in the γ parameter leads to reduced average distances between nodes, enhancing the likelihood of discovering shorter paths between them. However, this also results in diminished clustering coefficients and reduced tendencies of nodes to form groups and clusters.

The figure underscores the significance of degree distribution heterogeneity in relation to Milgram's condition and degrees of separation. Milgram's condition is notably influenced by network statistics and structural attributes such as clustering coefficients, degree distribution, and other topological factors. Consequently, the level of heterogeneity can impact how information propagates throughout the network and subsequently affect Milgram's condition. In the case of scale-free networks characterized by a power-law degree distribution, a few highly connected hubs coexist with numerous poorly connected nodes. These hubs assume a critical role in bridging various sections of the network and facilitating the transmission of information. As the degrees of separation, q, increase, the influence of larger cycles becomes more pronounced, and Milgram's condition is observed to exhibit an exponential decay pattern within this complex network model, deviating from the typical power-law regime.

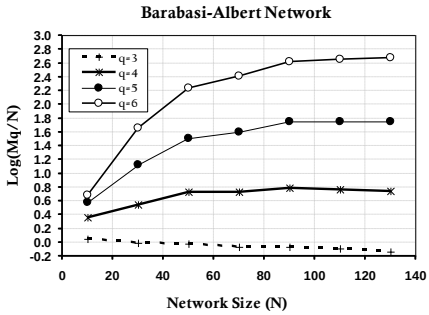

(a) Barabási-Albert (BA) model with scaling exponent γ~3

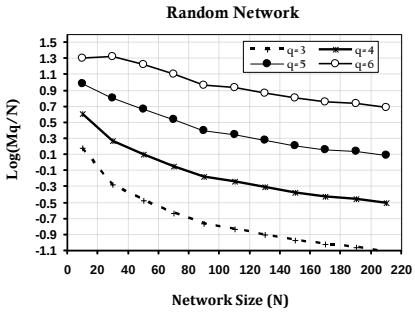

(b) Erdosh-Reiny (ER) random network with the probability connection of 0.4

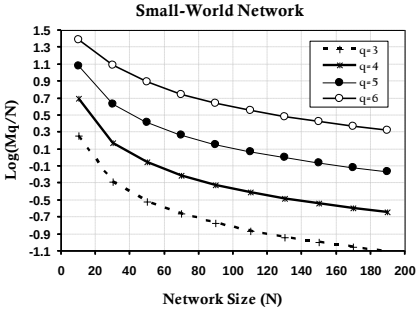

(c) Watts-Strogatz small-world model with rewiring probability α=0.3

Figure 7: Milgram's condition as a function of network size across various network models, encompassing random networks (ER), small-world networks (WS), and the Barabási-Albert model (BA).

The relationship between Milgram's condition and network size in various network models, such as random networks, small-world networks, Barabási-Albert model, and scale-free models, is illustrated in Figure 7. As previously discussed, Milgram's condition can be interpreted as a measure of network efficiency, indicating how effectively information can be transmitted across the network. The presence of walks and cycles in the network, as well as their frequency, increases the likelihood of effective communication between nodes, even if they appear to be distant from each other.

Further, we mentioned that the logarithm of Milgram's condition corresponds to the percentage of nodes in the network that can be reached within q-degree of separation and is of the same order of magnitude as the total number of nodes in the network. When the plots touch the line y=0.5, it signifies that the probability of two randomly chosen nodes communicating through q intermediate nodes is greater than 50%. With the increase in network size, the plots for random networks and the small-world model show a decrease in Milgram's condition, signifying a decrease in the likelihood of efficient communication and an increase in the degrees of separation. In smaller and medium-sized networks of such models, achieving 3- degree of separation is still possible. However, for larger networks, Milgram's condition can be met for 5 and 6 degrees of separation.

In contrast, in scale-free networks and Barabási-Albert model, Milgram's condition is met for 3- degree of separation only in smaller network sizes, which closely resemble small-world models. For larger sizes, Milgram's condition is met for $q \geq 4$ degrees of separation. This observation aligns with the previously discussed influence of network topology on Milgram's condition. While Milgram's condition can manifest in any network model, its precise location and behavior are influenced by various factors, including network size. The presence of highly connected hubs linked to numerous poorly connected nodes reduces Milgram's condition as the network size increases. Therefore, to satisfy Milgram's boundary condition, an increase in the degree of separation between network nodes is required.

Figure 8 illustrates Milgram's condition and its boundary conditions concerning the scaling exponent parameter, denoted as γ, in the scale-free network with specified characteristics. As explained in Equation (10), the logarithm of Milgram's condition serves

as a figure of merit (FoM) that quantifies the quality of communication within a network. It reveals how effectively information can be transmitted within q hops (degrees of separation) relative to the network's size. The intersection of the line y=1 with these plots indicates the saturation point. At this stage, the search process in Milgram's experiment has spread across the entire network, and the probability of finding the target node becomes very high. Conversely, the line y=0.5 (the median of the CDF) signifies the average degrees of separation in the network. For more than half of the nodes, there are, on average, q acquaintances with whom they can exchange messages. The likelihood of communication through q-degree of separation to connect with each other exceeds 50%, which is roughly half of the boundary condition (saturation point) observed in Milgram's experiment.

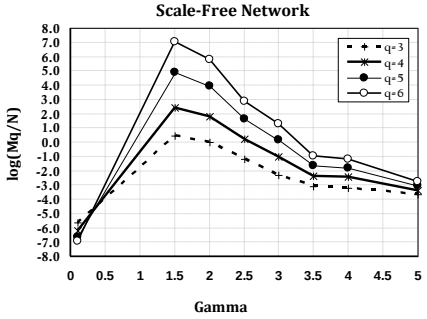

Figure 8: The Milgram's condition according to the scaling parameter, γ, of the power exponent, in the scale-free network with size 100.

Additionally, a lower parameter γ corresponds to shorter average path lengths and more straightforward information transmission. The plots in Figure 8 reveal that degrees of separation $q\geq4$ are associated with Milgram's boundary condition within the $2<\gamma<3$ regime, consistent with the scale-free network model. In this model, there are virtually no instances of 3-degree of separation for any value of the parameter γ. This phenomenon is a consequence of the emergence of giant hubs, explaining why degrees of separation q=4 to 6 are observed within the $\gamma\leq2$ regime. However, as $\gamma\geq3$, none of the degrees of separation, including q=6, can reach the boundary line. Nevertheless, within the power-law regime ($2<\gamma<3$), the degrees of separation of 5 and 6 can occur.

In the previous sections, we discussed the correlation between the q-degree of separation phenomenon and the rate of information propagation in networks. Now, we introduce a parameter called r_n, which relates to the q-degree of separation and the information transmission rate within the network. We define r_n as the ratio of the number of non-zero elements in the adjacency matrix of the graph to the total number of elements in the n^{th} power of the adjacency matrix, where $1\leq n\leq q$. It has shown that if this ratio equals 1 in a power of the adjacency matrix of the graph, it signifies that the search process is ergodic, and the graph is connected [23]. The corresponding Markov chain for this stochastic process is termed irreducible [23]. Therefore, in different network models, the quantity r_n can provide valuable insights into the connectivity of nodes within n hops (degrees of separation), where $1\leq n\leq q$. Essentially, the random variable r_n indicates the percentage of network nodes that can connect to each other with a maximum of q-degree of separation to exchange information and messages.

We can also define a cumulative distribution function, denoted as $T_q=\sum_{n=1}^{q} r_n$, for the random variable r_n. T_q represents the summation of the ratios of non-zero elements in the adjacency matrix to the total number of elements, encompassing degrees of separation from 1 to q. Essentially, this quantity signifies the cumulative likelihood of nodes that can be connected to each other within a maximum of q hops.

Figure 9 illustrates diagrams representing the percentage of nodes that can connect within a maximum of q hops (r_q) and their cumulative frequency (T_q) in scale-free network models based on the power-law scaling parameter, denoted as γ. In the regime where $\gamma\leq2$, owing to the presence of exceptionally large hubs and their dominance, as well as the contraction of average distances, it is observed that more than 80% of nodes can establish connections within two or three hops (degrees of separation). Within this range, it is evident that T_q exceeds unity, indicating a critical Milgram's condition. This signifies the occurrence of triangular relationships and their significant contribution in the $\gamma\leq2$ regime. In the scale-free regime of $2<\gamma<3$, it becomes apparent that for $q\geq4$ degrees of separation, more than 50% of nodes are capable of exchanging information and messages. In essence, under this regime, 3-degree separation scenarios do not occur. At the critical point γ=3 (Barabási-Albert model), the degrees of separation required to connect more than 50% of the nodes increase to 6 or more. In the $\gamma>3$ regime, the situation is analogous, and low degrees of separation are not observed in the network; instead, a minimum of 6-degree of separation (i.e., $q\geq6$) is necessary to meet Milgram's condition ($T_q>1$).

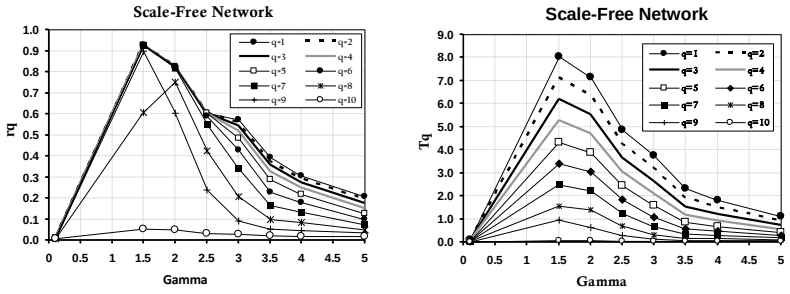

(a) (b)

Figure 9: (a) The percentage of nodes connected to each other within a maximum of q hops (r_q); (b) their cumulative frequency (T_q) in scale-free network model as a function of the scaling exponent parameter γ; the network size is set to 100 nodes.

4.2 The Milgram's Condition in Watts-Strogatz Small-World Model

In this section, we delve into the examination of the small-world phenomenon, Milgram's condition, and degrees of separation within the Watts-Strogatz network model through simulation experiments and the utilization of various metrics introduced in the article.

Figure 10 provides frequency histograms illustrating the cycles ranging from length 3 (triangles) to length 6 (hexagons) as a function of the rewiring probability, α, in the Watts-Strogatz small-world network model. Contrary to the initial expectation, it is evident that, for all values of rewiring probability α falling within the interval [0, 1], cycles with a length of 4 (squares) are more frequent compared to other cycle types. This phenomenon can be attributed to the dominance of cycles with a length of 4 in the small-world model. The explanation lies in the fact that the small-world model algorithm initiates with a regular lattice and subsequently performs random edge rewiring. A regular lattice inherently contains many cycles of length 4, so that the rewiring process primarily alters local connections. In such network, each node is typically connected to its k nearest neighbors, often chosen as an even number. When the rewiring probability α is low, only a small fraction of edges swapped over time, resulting in a network with high clustering. The increased frequency of cycles with a length of 4 can be attributed to the fact that each set of four neighboring nodes within the regular ring forms a square.

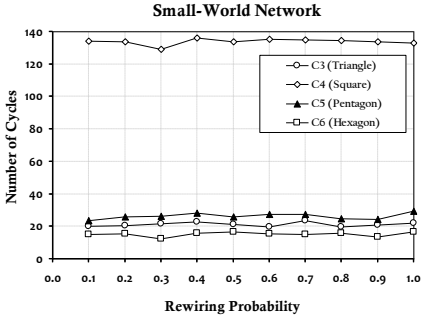

Figure 10: The frequency distribution of cycles with lengths ranging from 3 (triangles) to 6 (hexagons) as a function of the rewiring probability in the Watts-Strogatz small-world network model. This simulation involves a network consisting of 100 nodes.

As the rewiring probability $\alpha \to 1$, the local clustering in the network decreases, leading to a reduction in the number of squares (cycles with a length of 4). This reduction results in the emergence of longer cycles in the network. However, it is worth noting that even as the network's local clustering decreases, cycles of length 4 remain more prevalent than other cycle lengths. This observation aligns with the numerical simulation outcomes depicted in Figure 10. It is important to clarify that a high local clustering coefficient in the small-world model does not necessarily translate to a higher number of triangles. A high clustering coefficient indicates that neighboring nodes in the network have a strong tendency to connect with each other, facilitating message exchange. However, this clustering feature does not directly contribute to the presence of more triangles. Triangles are typically counted when calculating the clustering coefficient because they represent the simplest closed-loop structures in a network and can potentially form more complex network patterns. Therefore, triangles still exist due to high clustering, but the frequency of squares is higher because of the regular lattice structure in the initial network graph.

In summary, the frequency and lengths of cycles in the small-world model depend heavily on factors such as the algorithm of model generation, the characteristics of the initial regular network, and the extent of rewiring probability.

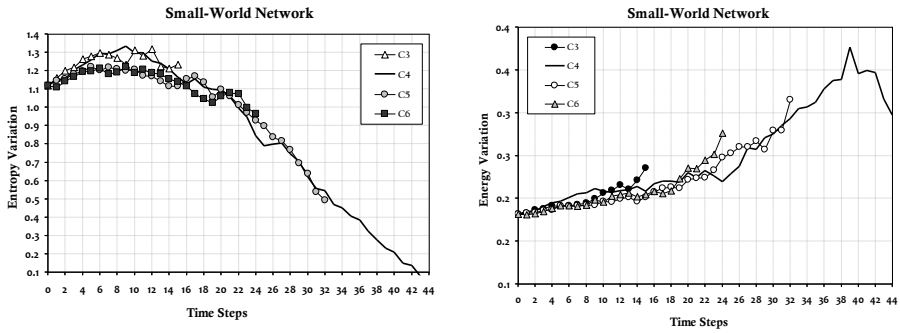

(a) (b)

Figure 11: The impact of removing cycles with lengths ranging from 3 to 6 (C_3 to C_6) on changes in spectral energy and graph entropy within the small-world network model. This analysis was conducted on a network comprising 100 nodes with a rewiring probability α set at 0.35. The removal of cycles, specifically those of lengths 3 to 6, is examined to understand its influence on two key network metrics: spectral energy and graph entropy.

In another experiment, we explored the consequences of removing cycles with different lengths, ranging from 3 to 6, on the entropy and spectral energy of the network. Figure 11 illustrates how removing these cycles impacts the graph's entropy and energy values within the context of the small-world network model. We conducted this investigation on a network consisting of 100 nodes, with a rewiring probability set at α=0.35. As evident from the diagrams, cycles play a significant role in altering the network's structure and influence its spectral and entropy properties. Notably, removing cycles with a length greater than 3 had a more pronounced effect on both the spectral energy and entropy of the network. This can be attributed to the fact that larger cycles contribute more to network connectivity. However, it is crucial to note that removing cycles may not necessarily lead to a decrease in the energy and entropy of the graph. Removing cycles could result in the creation of new cycles or disconnected components that alter the network's spectral properties.

The plots in Figure 11 highlight that the removal of cycles with a length of 4 (squares) had the most significant impact. This observation suggests that these cycles tend to form tightly connected subgraphs in the network, which can be thought of as modules or communities. Cycles of length 4 are often part of larger structures, such as cliques. Consequently, removing such cycles disrupts existing patterns in the network, reducing modularity and causing more fragmentation, resulting in fewer interconnections.

As depicted in the diagrams, removing cycles led to a reduction in network entropy. Among the various cycle lengths, removing squares had the most pronounced effect. This outcome aligns with the fact that cycles with a length of 4 were the most prevalent in the network. Additionally, while these tightly connected subgraphs facilitate information propagation within themselves (via short paths), removing them from the network leads to longer paths, reducing path diversity within the network. Consequently, this reduces the speed of information transmission among subgraphs. The diagram associated with cycles of length 3 (triangles) shows that, given their lower frequency, their removal had a smaller impact on entropy and energy changes in the graph. Reducing entropy values can also influence the phenomenon of degrees of separation and Milgram's condition. However, the extent of this influence is highly dependent on the network's specifications and its connection patterns. Hence, the subsequent sections of the article will delve into a detailed examination of the effect of various parameters on these network properties.

Another intriguing observation in the diagrams of Figure 11 is that, following the removal of cycles of varying lengths from the network, the graph's energy increased, in contrast to the entropy. This increase was particularly notable for cycles of length 4. This phenomenon can be attributed to the removal of cycles causing the network to become more heterogeneous and inducing structural changes. Consequently, these structural changes affected the spectral properties of the graph, which are highly sensitive to the network's structure. It is worth noting that this sensitivity to cycle removal is more pronounced in the entropy index. Thus, both graph entropy and energy serve as valuable indicators for explaining these structural alterations. Removing cycles introduced greater diversity in node degrees, leading to a decrease in entropy and an increase in graph energy.

One important takeaway from this observation is that when assessing the impact of cycle length on eigenvalues within a network model (such as the small-world model), indicators like the energy associated with the eigenvalues of the adjacency and Laplacian matrices can be effectively employed. This is because the adjacency matrix of a graph, which determines the eigenvalues and, consequently, the energy of the graph, exhibits a meaningful correlation with cycle lengths in the network. Further, transitioning from one network model to another and altering network topologies distinctly influences the distribution of eigenvalues. In different network models, metrics like the spectral gap and its relationship with high clustering can be measured. This relationship implies efficient communication and the ability to find effective paths between nodes. However, in graphs containing a significant number of short cycles, the spectral gap may be less significant, making it challenging to find optimal communication paths and exchange messages efficiently between nodes.

In the following sections, we will delve into various simulation experiments involving different network models and their statistics. The aim is to investigate how these statistics affect Milgram's condition and degrees of separation. For instance, by examining the impact of cycles, we can determine whether they create bottlenecks within the network, impeding efficient pathfinding and, consequently, affecting Milgram's condition.

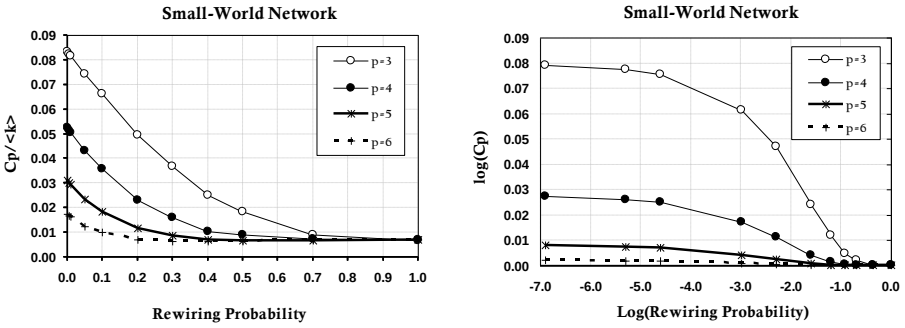

(a) (b)

Figure 12: (a) The plot illustrates the ratio of the generalized clustering coefficient to the average network degree, $C_p/\langle k\rangle$, as a function of the rewiring probability in the small-world model. The network size is held constant at 100 nodes; (b) the diagram displays the generalized clustering coefficients (C_p) according to the probability of rewiring in the small-world model, with both axes drawn in a logarithmic format. The network size and average degree are fixed.

Figure 12(a) presents diagrams illustrating the ratio of the average generalized clustering coefficient to the average degree, $C_p/\langle k\rangle$, as a function of the rewiring probability, α, in the Watts-Strogatz small-world model. The network size is kept constant. Moreover, Figure 12(b) shows the relationship between generalized clustering coefficients, C_p, and the rewiring probability α. Both axes in this plot are displayed in a logarithmic format.

Analysis of the diagrams reveals that as $\alpha\rightarrow 1$, and the network transitions towards a random network model, the generalized clustering coefficients decrease. In random networks, the clustering coefficient is directly proportional to the ratio of the average degree to the network size. Consequently, as the rewiring probability increases while maintaining a constant average degree, the generalized clustering coefficients decrease inversely proportional to the network size.

For small values of the probability α, the network model exhibits small-world behavior. Notably, the effect of cycles with a length of 3 (triangles) is significantly different from cycles with lengths ranging from 4 to 6. Among these, cycles with a length of 6 have the least impact and contribution. However, as the probability α increases, and the model approaches the dominion of random networks, the influence of cycle length diminishes. At this stage, cycles of various lengths exhibit similar contributions and are not significantly different from each other.

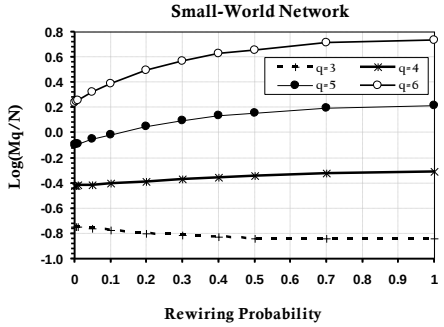

Figure 13: The Milgram's condition as a function of the rewiring probability, α, in the small-world model. The network size is kept constant, as is the fixed average degree.

Figure 13 presents the plots of Milgram's condition based on the rewiring probability, α, in the small-world model, while maintaining a constant average degree and a fixed network size of 100 nodes. The figure reveals that as $\alpha\rightarrow 1$, the network's behavior shifts towards that of a random network model. These diagrams demonstrate that, for low values of α (indicative of the small-world property), cycles of length 3 (triangles) or triangular clustering coefficients remain influential. In such scenarios, both high clustering and short paths coexist. At this stage, large clusters and giant components have not yet formed, resulting in a diminished contribution from longer cycles. It is important to note that the probability of such cycles' existence is proportional to $C_p(p+1)^{-\zeta}$ where ζ is the scaling parameter which controls the decay of clustering coefficients with respect to cycle length p. For low values of α, the ζ parameter is relatively larger, indicating that longer cycles contribute less to the clustering coefficients. However, as α increases and the network approaches the characteristics of random network models, $\zeta\rightarrow 0$. Consequently, there is a need to consider the contribution of longer cycles (moving away from the small-world property) in order to meet Milgram's boundary condition. These diagrams effectively illustrate the relationship between Milgram's condition and the network's topological structure in the small-world model.

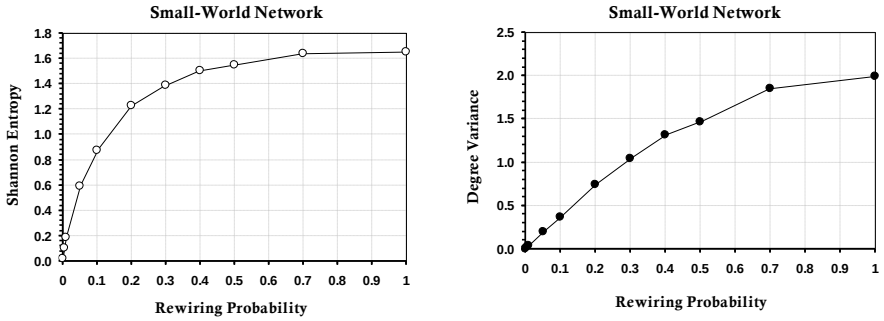

Figure 14: The plots of Shannon's entropy and the degree variance in relation to the rewiring probability, α, in the small-world model. The simulations maintain a constant network size of 100 nodes and a fixed average degree.

Figure 14 illustrates the changes in Shannon's entropy and degree variance as a function of the rewiring probability, α, in the Watts-Strogatz small-world network model. The diagrams clearly demonstrate how these network properties are influenced by variations in α. The Shannon entropy plot reveals that as $\alpha \rightarrow 1$ and the network transitions towards a more random structure, the entropy values also increase. This is an expected outcome, as higher α values indicate a departure from the small-world network configuration, leading to increased randomness and disorder in the network. The degree variance measures the variability in node degrees within the network. The plot for degree variance shows a significant increase as $\alpha \rightarrow 1$, signifying a shift towards a random network model. In contrast, for smaller α values, the network displays lower degree variance, indicating a more uniform distribution of node degrees.

Overall, these results align with expectations. Small-world networks, characterized by lower α values, exhibit properties resembling regular networks, including lower entropy, lower degree variance, and shorter degrees of separation. As α increases, the network transitions towards a random model, resulting in higher entropy, greater degree variance, and a need for larger degrees of separation to fulfill Milgram's condition. This transition reflects the changing network topology and the reduced prevalence of cyclic structures and clustering, which play a role in connecting different parts of the network in the small-world regime.

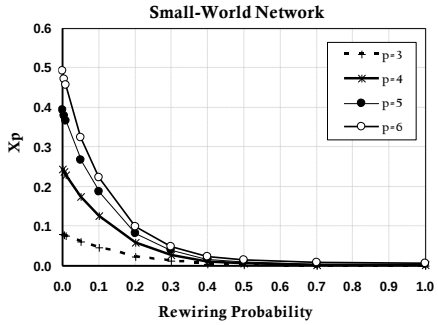

Figure 15: The cumulative frequency of generalized clustering coefficients, denoted as X_p, as a function of the rewiring probability, α, in the Watts-Strogatz small-world network model while keeping the network size constant at 100 nodes and maintaining a fixed average degree.

In Figure 15, the cumulative frequency of cycles' contributions with different lengths, spanning from 3 to 6 (summation the generalized clustering coefficients, C_p), is depicted with respect to various values of the rewiring probability α in the Watts-Strogatz small-world network model. The diagrams illustrate how the cumulative frequency of C_p changes as α varies.

For small values of α, indicating adherence to the small-world phenomenon, the contribution and impact of cycles with a length of 3 (triangles) are more prominent (as indicated in Table 2). However, as $\alpha \rightarrow 1$ and the network gradually transitions towards a more random configuration, the contribution of cycles decreases significantly and falls below 20%. Nevertheless, in most cases, larger cycles continue to make a more substantial contribution.

In situations where α takes on large values, and the network behaves like a random model with an average distance proportional to $\ln N$, the degree variance is constrained because there are no extensive clusters that influence the degrees of separation. Consequently, the extent of the contribution of cycles becomes roughly similar among different cycle lengths.

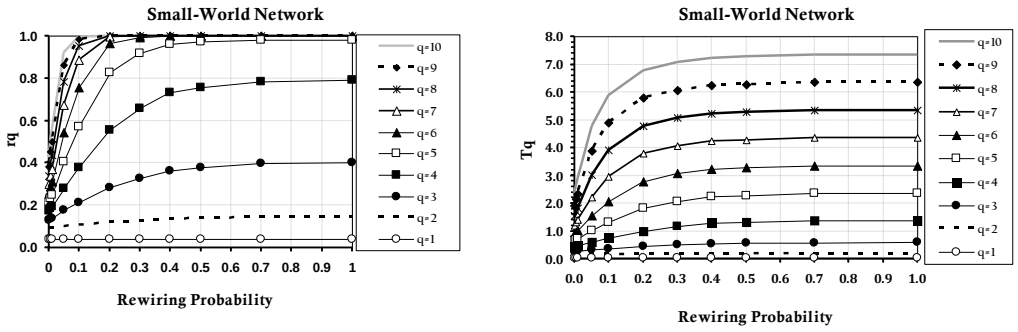

(a) (b)

Figure 16: Two sets of diagrams related to the Watts-Strogatz small-world model; (a) the percentage of nodes connected to each other after a maximum of q hops (r_q); (b), the cumulative frequency, T_q. The measurements are depicted concerning different values of the rewiring probability. The network's average degree is kept constant, and the network size remains fixed at 100 nodes.

Figure 16 provides plots for the random variable r_n , $1 \le n \le q$, and its cumulative frequency, T_q, within the Watts-Strogatz small-world network model, with variations in the rewiring probability α. In this context, r_n represents the percentage of network nodes that can connect to each other within n hops, facilitating the exchange of information and messages. The quantitiy T_q, on the other hand, represents the cumulative frequency, signifying the summation of the probability of nodes connecting to each other within a maximum of q steps.

The diagrams demonstrate that in the small-world model, particularly for low rewiring probabilities, nodes connect to each other quickly within a few hops. For instance, with a rewiring probability of 10%, nearly 50% of the network nodes can be interconnected after 6 hops. An intriguing observation is that the condition $T_q>1$, analogous to Milgram's boundary condition, is met when the rewiring probability is at 10% and $q \ge 5$. However, for $q \le 4$, under most circumstances, increasing the rewiring probability does not lead to the satisfaction of $T_q > 1$. This implies that the cumulative frequency reaches the saturation point, where almost all network nodes are reachable after q-degree of separation, primarily for $q \ge 5$.

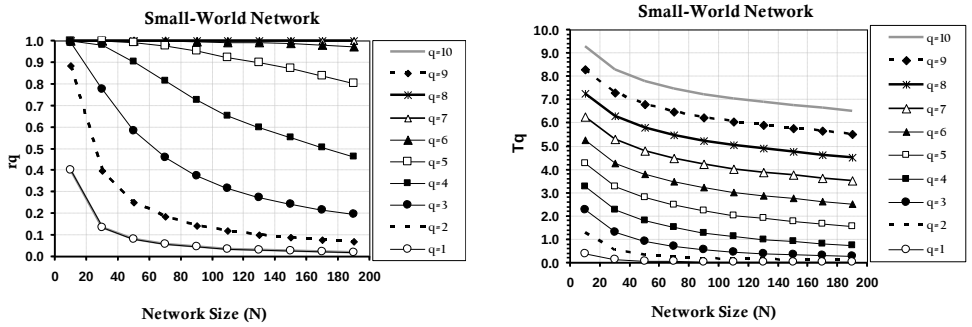

(a) (b)

Figure 17: (a) the plots depicting the percentage of nodes connected to each other within a maximum of q hops (r_q); (b) their cumulative frequency (T_q) in Watts-Strogatz small-world networks. The plots illustrate the impact of varying network sizes while keeping the rewiring probability α constant at 0.3 and assuming a fixed average degree for the network.

The plots in Figure 17 reveal the impact of network size on the Watts-Strogatz small-world model. In these networks, it becomes evident that after reaching q=3 degrees of separation, nearly all network nodes become accessible to each other. Moreover, for $q \ge 3$, the Milgram's boundary condition of $T_q>1$ is met. This observation underscores the significance of triangular relationships in establishing the small-world effect, particularly in relatively small networks. However, as the network size increases, the relative contribution of such triangular relationships decreases significantly. The plots also highlight that in larger small-world networks, more than half of the nodes are connected within $q \ge 4$ degrees of separation. This reinforces the notion that the fulfillment of Milgram's condition for a 3-degree separation is feasible primarily in smaller small-world networks. For larger networks, it becomes possible to meet Milgram's condition with higher degrees of separation.

The emergence of clusters and larger groups of nodes, along with a substantial number of poorly connected nodes, contributes to the decrease in Milgram's condition as network size increases. Consequently, to meet Milgram's condition, increasing the degrees of separation between network nodes becomes a necessity as network size grows.

4.3 Hamming Distance and Network Multiplicity

In this section, we will explore the coefficients and average Hamming distance in network models and their relationship with Milgram's condition and degrees of separation. The Hamming distance is employed as a measure of distance instead of the traditional average distance index. This metric is associated with concepts such as network heterogeneity, network energy, and the reduction of the resistance distance in a graph, ultimately enhancing conductivity and the speed of information propagation in the network. The

Hamming distance is a measure that quantifies the difference between two sequences of equal length. It is commonly used in information theory and coding [24].

In graph theory, the Hamming distance can be applied to compare two graphs based on their adjacency matrices. To compute the distance and the average Hamming distance within a graph, one can utilize either the adjacency or the incidence matrix. This distance represents the number of positions where corresponding entries differ in the adjacency matrix (incidence matrix) of the graph. Essentially, it corresponds to the number of edges that must be added or removed to transition from one vertex to another. The average Hamming distance can be determined by summing the Hamming distances across all pairs of graph vertices and then dividing this sum by the total number of vertex pairs. Consequently, the Hamming distance signifies the number of edges that differ between vertices. This measure is heavily influenced by the quantity and arrangement of edges within the graph and can be viewed as the expected value of the probability that two n-bit strings differ in some positions. This is why the Hamming distance is occasionally referred to as the error probability in coding theory [24], as it serves as a measure for estimating the distance (difference) between code words in error detection and correction codes.

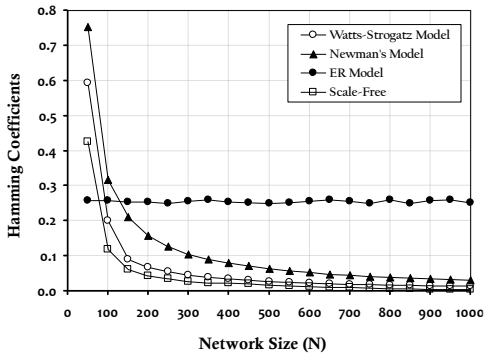

Figure 18: The Hamming distances as a function of the number of nodes (network size) in various network models. These models include the Watts-Strogatz small-world [3] with a rewiring probability α= 0.3, the Neumann model [11], the random ER model [7] with a connection probability of 0.4, and the scale-free model [6] with a scaling exponent γ= 2.5.

Figure 18 illustrates the Hamming distances concerning the number of nodes (network size) in different network models. In the Watts-Strogatz small-world network, a rewiring probability of 0.3 is applied, in the Neumann model [11], in the random ER model [7], the connection probability is set at 0.4, and in the scale-free model [6], the scaling exponent is assumed to be γ=2.5.

Observing the plots, it is evident that as the network size increases, the Hamming distance experiences an exponential decrease. This reduction is particularly pronounced in scale-free networks compared to other models. An intriguing observation is that in the case of random networks, the Hamming coefficients remain relatively constant and nearly equal to $\langle k\rangle/n(2n-\langle k\rangle)$, where $\langle k\rangle$ represents the average degree of the network. The decrease in the Hamming coefficient and the increase in network multiplicity suggest that more nodes share the same Hamming distance.

Scale-free networks, even with increasing size, continue to exhibit the lowest Hamming distance among all the models. This phenomenon can be attributed to the relatively close proximity of nodes in scale-free networks, resulting in higher connectivity.

Additionally, a measure called multiplicity in a network can be defined in terms of Hamming distance.

$$M = 1 - D_h / D_n \tag{15}$$

The parameter D_h represents the internal Boolean product of two vectors, specifically rows i and j, of the network's adjacency matrix. On the other hand, D_n stands for the Hamming distance, which quantifies the distance between all pairs of vectors. In random networks, D_h can be interpreted as the mathematical expectation (average probability) that the i^{th} element in a row (an n-bit string consisting of zeros and ones) differs from another n-bit string in the i^{th} position bit. Essentially, D_h measures the average Hamming distance between pairs of rows in the adjacency matrix, indicating the average number of distinct elements between two rows.

Therefore, M is a criterion, gauges the level of similarity between rows of the adjacency matrix. This metric is normalized relative to the maximum possible difference, D_n. Consequently, M falls within the range of 0 (when all pairs of rows are entirely dissimilar) to 1 (when all pairs of rows are identical).

In the case of a regular network, where D_n equals $n-1$, all nodes have the same degree, and each row of the adjacency matrix is similar to the others. Therefore, the Hamming distance between all pairs of vertices is equal to $n-1$. In other words, in a regular graph, every vertex has the same degree, which implies that each row of the adjacency matrix contains the exact same number of 1s.

If the degree of each node is denoted as k, then for arbitrary rows i and j in the adjacency matrix, there are only two possibilities: either they are identical, resulting in a Hamming distance of zero, or they differ in precisely one position, indicating the presence of an edge between nodes i and j. In this latter case, the Hamming distance is equal to 1. Due to the regularity of the graph, each row has exactly k ones. This means that it differs from every other row in exactly k positions. Therefore, any two arbitrary rows i and j must be distinct in exactly k positions. In a regular graph, k is equal to $n-1$, as each node is connected to all other nodes except itself. Consequently, the total number of edges in the graph is $kn/2$, and the Hamming distance between two rows in a regular graph equals $n-1$.

The multiplicity parameter *M* carries additional significance in the context of graph theory. It is linked to the number of times an eigenvalue appears as a root of the characteristic polynomial of the adjacency matrix. Consequently, it can provide valuable insights into both the geometric and algebraic properties of the graph. Further, *M* can be interpreted as a measure of redundancy within the graph, indicating that each eigenvalue may appear multiple times in the graph's spectrum.

An interesting point to highlight is that the multiplicity criterion, based on Hamming distance, serves as a similarity measure between two vectors (rows) within the adjacency matrix. Higher values of *M* signify a greater degree of similarity between two vectors, which can be viewed as a strong level of connectivity and acquaintanceship between the nodes represented by these vectors. From the perspective of degrees of separation, the *M* criterion can offer valuable insights into network connectivity. For instance, if *M* is calculated for all pairs of nodes in the network and a substantial number of pairs exhibit high values, it suggests that numerous nodes in the network are closely interconnected. This interconnectedness results in a reduction in the average distance and shorter paths between nodes.

Indeed, while the multiplicity criterion based on Hamming distance offers insights into network connectivity and similarity between nodes, it represents just one facet of a comprehensive analysis of network structure. To gain a thorough understanding of a network's properties and its influence on information propagation, degrees of separation, and overall behavior, it's crucial to consider this criterion alongside other key metrics such as average distance, clustering coefficient, and degree distribution. These combined insights provide a more holistic view of a network's characteristics and functionality.

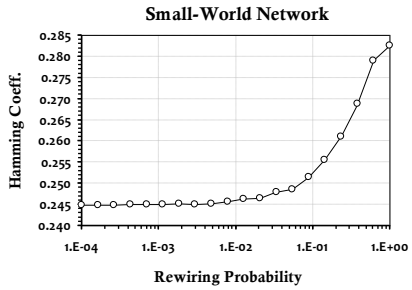

Figure 19: The Hamming coefficients as they relate to the probability of rewiring in small-world networks. The network size in this context consists of 100 nodes, and the horizontal axis is represented on a logarithmic scale. The Hamming coefficients are used to measure the degree of similarity or difference between networks' configurations as rewiring probabilities vary. This figure likely demonstrates how the Hamming coefficients change across different rewiring probabilities in small-world networks with 100 nodes.

Figure 19 demonstrates the variation in Hamming distance with respect to the rewiring probability in small-world networks. The average degree is fixed and the number of nodes is set to 100. The key observations from this figure are as follows. As the rewiring probability, α, increases, the network transitions toward a more random structure. This shift is associated with a significant increase in Hamming coefficients. For low values of α, the network's structures are highly similar, resulting in small Hamming distances between nodes. Consequently, the multiplicity parameter values are high, indicating that many pairs of nodes share similar network configurations. Conversely, as $\alpha \rightarrow 1$, the similarity among network structures diminishes. This leads to a sharp decrease in the number of node pairs with low Hamming distances, ultimately resulting in an increase in the overall Hamming distance.

In summary, this figure highlights how changes in the rewiring probability impact the structural similarity of small-world networks. Lower rewiring probabilities result in networks with more similar structures, while higher probabilities lead to increased structural diversity and higher Hamming distances between nodes.

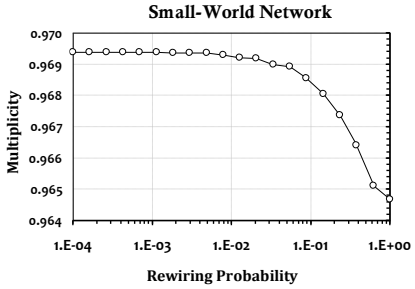

Figure 20: The multiplicity parameter, *M*, as a function of the rewiring probability, α, in the small-world network model. The network size is fixed at 100 nodes, and the horizontal axis is logarithmic.

Figure 20 illustrates the plot of the multiplicity parameter, *M*, concerning the rewiring probability, α, in the Watts-Strogatz small-world network with a size of 100 nodes. As evident, as $\alpha \rightarrow 1$, the network tends towards randomness, leading to a rapid decrease in the *M* index. It is important to note that the impact of edge swapping and the rewiring mechanism on the *M* parameter heavily relies on the specifics of the employed rewiring mechanism. In this context, we utilized the rewiring technique associated with the Watts-Strogatz model [3]. However, the application of random rewiring—although it partially preserves certain network characteristics like the degree distribution or clustering coefficient—also results in a swift reduction in *M* values. This is because it disrupts similarity patterns and common neighbors among nodes in the network.

In Equation (15), the parameter D_h denotes shared features or common neighbors between two nodes, while D_n represents the total number of differences between these nodes. Consequently, the M criterion can be interpreted as the percentage of shared information among interconnected nodes. Higher M values signify greater levels of similarity between nodes, which can potentially facilitate efficient information propagation within the network.

It is worth acknowledging that M exhibits an inverse relationship with the Hamming distance (refer to Figures 19 and 20) and can determine the number of node pairs in the graph with a specific Hamming distance. This knowledge proves valuable for estimating metrics such as degrees of separation, network diameter, as well as the spectral properties of the graph. In cases where the graph boasts high multiplicity and low Hamming distance, it indicates that the nodes within the graph are strongly interconnected. Conversely, as the Hamming distance increases and multiplicity decreases, the graph portrays nodes that are relatively distant from each other, resulting in reduced connectivity.

The multiplicity measure is also intricately linked to the average network geodesic distance. When the average distance decreases and the Hamming distance increases, the network's multiplicity decreases as well. A decrease in the average distance implies that there are more short paths connecting graph vertices, consequently increasing the number of vertex pairs with low Hamming distance. As previously mentioned, the clustering coefficient quantifies how strongly vertices tend to form clusters and communities. Higher multiplicity corresponds to increased clustering and a smaller average distance. Conversely, this relationship works in the opposite direction too. In random networks characterized by low clustering coefficients and higher average distances, a reduction in the multiplicity criterion is observed.

High multiplicity in structures like Neumann's model [11] or the Watts-Strogatz small-world network [3] signifies the presence of numerous diverse and alternative routes between nodes, facilitating and expediting the flow of information throughout the network. The coexistence of low average distances and high clustering coefficients in such models indicates that the network exhibits both local and global connectivity. When Hamming distance is low and multiplicity is high, more pronounced small-world properties emerge. Multiplicity implies the existence of numerous alternative routes between nodes, easing information flow within local clusters and shortcuts connecting different regions in the network. Networks with high clustering coefficients possess many cycles of length 3 (triangles), resulting in low Hamming distance and high multiplicity. In summary, since multiplicity can be seen as a measure of path diversity or redundancy between nodes in the network, it significantly impacts degrees of separation and Milgram's condition. Therefore, parameter M can be related to Milgram's condition, the frequency, and the length of cycles ranging from 3 to 6. When a network exhibits high multiplicity, it implies more overlap between the neighbors of interconnected nodes, fostering the formation of cycles and shorter paths between nodes. Consequently, a greater number of alternative and potential paths between nodes facilitates faster information propagation and fewer degrees of separation.

Table 1: Numerical values of the real-world network measures

Measures		Real-world Networks									
		Network Virology (COVID-19) [28]						Chesapeake [29]	Zachary's karate club [27]	ASD [30]	TD [30]
		Alpha	Beta	Omicron		Gamma	Delta				
				BA.1	BA.2						
No. of nodes (N)		289	289	289	289	292	290	39	33	100	100
No. of Edges (L)		1009	1026	996	1035	1039	1004	170	78	73	116
C3		0.45	0.45	0.45	0.44	0.44	0.44	0.28	0.255	0.52	0.52
C4		0.27	0.28	0.27	0.27	0.27	0.27	0.37	0.259	0.42	0.40
C5		0.17	0.18	0.18	0.17	0.18	0.17	0.29	0.169	0.35	0.32
C6		0.12	0.12	0.12	0.11	0.12	0.12	0.29	0.134	0.28	0.24
Average Distance (<d>)		6.084246	5.872141	6.153547	5.893527	5.956056	6.043622	1.83	2.4082	1.22	1.67
Ln(N)		5.66642	5.66642	5.66642	5.66642	5.67675	5.66988	3.663	3.4956	4.6051	4.6051
Rate of Information (R)		0.070557	0.070557	0.070557	0.070557	0.071289	0.070801	0.009	0.008301	0.01	0.01
Average Degree (<k>)		6.982699	7.100346	6.892734	7.16263	7.116438	6.924138	8.71	4.588235	2.39	3.17
Diameter (dmax)		16	16	18	15	14	16	3	17	1.625	2.889
Heterogeneity-index [25]		0.0209	0.0212	0.0223	0.0217	0.0227	0.0221	0.288	0.051	0.007	0.006
rq	q=3	0.292753	0.304822	0.285617	0.311598	0.306319	0.294126	1	0.986159	0.15	0.17
	q=4	0.435902	0.459657	0.427162	0.464566	0.456136	0.44126	1	1	0.17	0.19
	q=5	0.58353	0.618084	0.571557	0.616312	0.606258	0.593246	1	1	0.17	0.20
	q=6	0.716047	0.752709	0.704362	0.744615	0.736771	0.726326	1	1	0.17	0.21
Tq	q=3	0.566732	0.58438	0.552951	0.59961	0.588103	0.56635	3.15	2.581315	0.38	0.45
	q=4	1.002634	1.044037	0.980113	1.064175	1.044239	1.00761	4.15	3.581315	0.55	0.65
	q=5	1.586164	1.662121	1.55167	1.680488	1.650497	1.600856	5.15	4.581315	0.73	0.86
	q=6	2.302211	2.41483	2.256031	2.425103	2.387268	2.327182	6.15	5.581315	0.91	1.07
Degree Variance		4.78	5.25	5.13	5.08	5.34	4.97	38.73	15.03	4.10	4.78
Milgram's Condition Log(Mq/N)	q=3	2.12	2.14	2.12	2.15	2.15	2.12	1.61	1.023	0.65	0.92
	q=4	2.93	2.96	2.92	2.97	2.97	2.92	2.57	1.67	1.23	1.48
	q=5	3.72	3.76	3.71	3.77	3.77	3.72	3.55	2.34	1.79	1.99
	q=6	4.51	4.56	4.5	4.50	4.57	4.5	4.47	2.93	2.29	2.42
Z-Estrada [17]	<Zpp>	4.26×10^{13}	9.96×10^{13}	9.67×10^{12}	3.68×10^{13}	4.65×10^{13}	7.92×10^{12}	2.88×10^{27}	4.40×10^{8}	1.82×10^{6}	1.60×10^{6}
	<Zpq>	1.32×10^{13}	2.48×10^{13}	3.62×10^{12}	1.81×10^{13}	1.90×10^{13}	3.43×10^{12}	2.34×10^{27}	3.10×10^{8}	3.43×10^{5}	2.51×10^{5}
Multiplicity (M)		0.980	0.979	0.980	0.979	0.979	0.980	0.929	0.882	0.99	0.998
Hamming_Distance		0.162	0.169	0.159	0.171	0.168	0.159	0.764	0.941	0.123	0.162
Scaling Exponent (γ)		3.5	3.5	3.5	3.5	3.5	3.5	3.5	2.16	1.98	1.98
Energy_Index [26]		0.291	0.725	0.284	0.288	0.295	0.283	0.587	0.554	0.336	0.391
Shannon Entropy		0.022	0.287	0.021	0.021	0.022	0.022	0.162	0.269	0.046	0.081

Up until now, we have utilized datasets based on three well-known random network models [7], small-world models [3], and scale-free models [6], all of which are synthetically generated. However, to gain a deeper understanding of the small-world phenomenon and Milgram's condition, and to assess the effectiveness of the approaches discussed in this article experimentally, we have applied the criteria [25, 26] on datasets [27-30] obtained from real-world networks spanning various domains such as biology, technology, and information. The numerical results extracted from these real-world networks are presented in Table 1. Our objective is to demonstrate the efficacy of the criteria introduced in this article for assessing degrees of separation and Milgram's condition, and to what extent these concepts can be empirically verified in real-world networks. This collection includes 10 real datasets: Zachary's karate club [27], C. elegans [27], various variants of COVID-19 (including Omicron [BA1, BA2], Alpha, Beta, Delta, and Gamma [28]), the Chesapeake network [29] (a type of food web network), and brain networks, specifically typically developed (TD) and autism spectrum disorder (ASD) [30]. All these networks represent a wide array of complex biological, informational, social, and technological systems. The details and specifications of these networks, along with the numerical values of various criteria, are calculated and presented in Table 1.

As observed, clustering coefficients in biological networks, such as brain and virology networks tend to be higher compared to other network types. Additionally, these networks exhibit lower levels of heterogeneity. In the case of various COVID-19 variants, parameter r_q values for $q\geq3$ have exceeded 60%, indicating that more than 60% of nodes (residues) in different COVID-19 variants can be connected within 3 to 4 degrees of separation to exchange information. Furthermore, the cumulative frequency value of T_q exceeds 1 for $q\geq4$, signifying the total likelihood of residues being able to connect within 4 hops.

Moreover, when fitting a regression line to the degree distribution data of such networks, it is evident that their scaling exponent follows $\gamma=3.5$. We previously discussed that when $\gamma>3$, the contribution of long-range cycles decreases, and the network converges towards a random model. The numerical data presented in Table 1 for the average distance of COVID-19 variants indicates that in these networks, the average distance scales proportionally to $\ln N$ (the natural logarithm of network size). Additionally, hubs are smaller, and the degree variance is limited. In other words, hubs do not exert a significant influence on degrees of separation but rather serve to reduce distances between residues. Consequently, these findings suggest that residue networks associated with COVID-19 variants align well with the small-world model.

In Section 3.1, we discussed how various factors influence the speed of information propagation within a network. To quantify the rate of information propagation, we introduced the *R*-index and the *Z*-Estrada parameter [17, 13]. Notably, the *Z*-Estrada parameter is particularly effective at capturing the information transfer capacity in small-world networks due to its ability to account for longer walks. When comparing the numerical results of the *Z*-Estrada parameter for different COVID-19 variants, a striking observation emerges. The values of the *Z*-Estrada for the Omicron variant are significantly higher than those for other variants, particularly the Delta variant. This observation provides valuable insights into why the Omicron variant exhibits a much higher rate of spread and contagiousness compared to other COVID-19 variants.

5. Conclusions, Directions, and Future Work

In this paper, we conducted a thorough exploration of the concept of degrees of separation and Milgram's condition in various complex network models, including random, small-world, and scale-free networks, from multiple perspectives and using various criteria. We presented an in-depth analysis that brings together previously unreported findings in a comprehensive manner. Our investigation encompassed the interplay between degrees of separation and other network statistics, such as average clustering coefficients and generalized clustering coefficients for cycles of different lengths, as well as the relationship between cycles and degrees of separation. Additionally, we examined the information propagation rate and its correlation with degrees of separation, considering different network topologies. We delved into the connection between degrees of separation and network heterogeneity, while also analyzing the impact of Hamming distance and the multiplicity criterion on degrees of separation and Milgram's condition. The numerical results derived from simulation outcomes clearly demonstrated that the presence of cycles of varying lengths within a network has a discernible impact on degrees of separation and Milgram's condition. We also observed direct relationships between Milgram's condition and both the clustering coefficient and the scaling exponent in the power-law regime in the scale-free network model. Furthermore, we highlighted the role of rewiring probability in small-world networks concerning degrees of separation. Our detailed examination of the multiplicity factor and Hamming distance shed light on their influence on the small-world phenomenon. Consequently, this article has contributed a comprehensive overview of degrees of separation and Milgram's condition in the context of complex networks, offering insights into potential applications across various domains.

Indeed, while this study has provided valuable insights into degrees of separation and Milgram's condition in complex networks, there remain numerous avenues for future research that warrant exploration. One intriguing direction is to investigate how community structures and modularity within networks influence degrees of separation, as well as their potential impact on information propagation and network resilience. In addition, delving into the realm of temporal dynamics and evolving networks could yield significant findings in this field. Applying the concepts and models discussed here to real-world small-world networks, including social, transportation, virology, and biological networks, among others, can offer valuable insights into the mechanisms and factors governing information flow within these systems. Evaluating network resilience and robustness against random failures and systematic attacks, with a specific focus on Milgram's condition and degrees of separation, is another promising avenue for future research. Additionally, it would be worthwhile to explore the influence of other criteria, such as weak ties and bridging nodes, on complex network properties and their relationship with degrees of separation and Milgram's condition. These directions hold the potential to expand our understanding of information dissemination and network dynamics in complex systems.

Declarations

Ethical Approval This article does not contain any studies with animals or human performed by any of the authors.

Competing interests The authors declare that they have no conflicts of interest.
Authors' contributions F. Safaei formulated the primary framework and wrote the article. M. R. Sadeghi conducted the simulation experiments, while M. Emadi Kochack was responsible for preparing the simulation results into visual representations, including figures and tables. All authors reviewed the manuscript.
Funding No funding was received from anywhere or anyone for this research.
Availability of data and materials The data that support the findings of this study are available from the corresponding author upon reasonable request.

References

[1] F. Karinthy, Chain-links, Everything is different, pp.21-26, 1929.
[2] S. Milgram, The small world problem, Psychology today, Vol. 2, No. 1, pp.60-67, 1967.
[3] D. J. Watts and S. H. Strogatz, Collective dynamics of small-world networks, Nature, Vol. 393, No. 6684, pp. 440-442, June 1998.
[4] A- L. Barabási and et al., Emergence of Scaling in Random Networks, Science, Vol. 286, No. 5439, pp. 509-512, 1999.
[5] R. Albert and et al., Statistical mechanics of complex networks, Reviews of Modern Physics, Vol. 74, No. 1, pp. 47-97, 2002.
[6] A.-L. Barabási, Network science, online book, available on *http://networksciencebook.com*/, visited 2025.
[7] P. Erdös and A. Rényi, On the Evolution of Random Graphs, Publications of the Math. Inst. of the Hungarian Academy of Sci., Vol. 5, pp. 17-61, 1960.
[8] Number of Facebook users worldwide from 2015 to 2020, Statista, available on ttps://www.statista.com/statistics/490424/number-of-worldwide-facebook-users/
[9] R. Caers et al., Facebook: A literature review, New media & society, Vol. 15, No. 6, pp.982-1002, 2013.
[10] *https://research.facebook.com/blog/three-and-a-half-degrees-of-separation*/, visited on 2023.
[11] M.E. Newman, Models of the small world, Journal of Statistical Physics, 101, pp.819-841, 2000.
[12] Bringmann, Karl, et al., Greedy routing and the algorithmic small-world phenomenon, Journal of Computer and System Sciences 125: 59-105, 2022.
[13] Reza Gholi Famian, Ali., A socio-semiotic approach to Small World Phenomenon in urban linguistic landscapes; A case study of Tehran, Language Research 15.1: 123-145, 2024.
[14] Goodrich, Michael T., and Evrim Ozel., Modeling the small-world phenomenon with road networks., Proceedings of the 30th International Conference on Advances in Geographic Information Systems, 2022.
[15] Schnettler, Sebastian., Small World, Handbuch Netzwerkforschung. Wiesbaden: Springer Fachmedien Wiesbaden, 1-11, 2023.
[16] Wu, Jiang., Small World in Social Networks, Social Network Computing. Singapore: Springer Nature Singapore, 219-256, 2024.
[17] E. Estrada, and et al., Communicability angle and the spatial efficiency of networks, SIAM Review, Vol. 58, No. 4, pp.692-715, 2016.
[18] E. Estrada, Topological analysis of SARS CoV-2 main protease, Chaos: An Interdisciplinary Journal of Nonlinear Science, Vol. 30, No. 6, 2020.
[19] N. Toyota, p-th Clustering coefficients Cp and Adjacent Matrix for Networks: Formulation based on String, arXiv preprint arXiv:0912.2807, 2009.
[20] F. Safaei, et al., A method for computing local contributions to graph energy based on Estrada–Benzi approach, Discrete Applied Mathematics, 260, pp.214-226, 2019.
[21] I. Gutman, The energy of a graph, Ber. Math.–Statist. Sekt. Forschungsz. Graz, 103, pp. 1-22, 1978.
[22] N. Toyota, Separation Number and Generalized Clustering Coefficient in Small World Networks based on String Formalism, arXiv preprint arXiv:1109.6719, 2011.
[23] G. Dewakar, Performance Appraisal and Compensation Management: A Modern Approach, Prentice-Hall, India Learning Private Limited, Jan. 2008.
[24] J. S. Chitode, Information Theory and Coding: Information, Source Coding and Channel Coding, Technological Publications, 2021.
[25] E. Estrada, Quantifying network heterogeneity, Physical Review E, Vol. 82, No. 6, p.066102, 2010.
[26] F. Safaei, S. Tabrizchi, A.H. Rasanan, M. Zare, An energy-based heterogeneity measure for quantifying structural irregularity in complex networks, Journal of Computational Science, Vol. 36, p.101011, 2019.
[27] Original website online: *http://www-personal.umich.edu/~mejn/netdata/*, visited 2025.
[28] Protein Data Bank, available on *https://www.rcsb.org/*, visited 2025.
[29] *http://cosinproject.eu/extra/data/foodwebs/WEB.html*, visited 2025.
[30] M. Zare, et al., Automatic classification of 6-month-old infants at familial risk for language-based learning disorder using a support vector machine, Clinical Neurophysiology, Issue 127, pp. 2695-2703, 2016.

Farshad Safaei received the B.*Sc*., M.*Sc*., and Ph.D. degrees in Computer Engineering from Iran University of Science and Technology (IUST) in 1994, 1997 and 2007, respectively. He is currently an associate professor in the Department of Computer Science and Engineering, Shahid Beheshti University, Tehran, Iran. His-research interests are Performance Evaluation of Computer Systems, Networks-on-Chips, and Complex Networks.
Email: f_safaei@sbu.ac.ir
Orcid Code: 0000-0002-8546-3148
Office phone: +9821-22904183
Cellular phone: +989123893561

Mohammadreza Sadeghi received his Bachelor’s degree in Computer Engineering from Shahid Beheshti University in 2023. Currently, he is pursuing his Master’s degree in Computer Science and Engineering, Applied Computing, at University of Oulu. His research interests are Optimization Algorithms, Graph Theory, and Human-Computer Interaction.
Email: mohammadreza.sadeghi@oulu.fi
Orcid Code: 0009-0000-1782-9155
Office phone: -
Cellular phone: +358417235690

Mohammad Mehdi Emadi Kouchak obtained his Bachelor's degree in Computer Engineering, Hardware, from the Islamic Azad University, South Tehran Branch in 2015. He further received his Master's degree in Computer System Architecture from the Islamic Azad University, South Tehran Branch in 2018. Currently, he is a Ph.D. student in Computer System Architecture at the Islamic Azad University, Science and Research Branch. His-research interests revolve around Complex and Social Networks, Design of Deep Learning Accelerators, and Quantum Computing.
Email: m.m.emadi@srbiau.ac.ir
Orcid Code: 0009-0009-2572-3356
Office phone: -
Cellular phone: +989127981452